Abstract

Reduced ice growth

Antifreeze(glyco) proteins (AF(G)Ps) are potent ice recrystallisation inhibitors (IRIs). However, their highly challenging synthesis and low availability means synthetic mimetics of AF(G)Ps are desirable. The most potent synthetic mimetic currently reported is poly(vinyl alcohol) (PVA). Since its first report in 1994, the mechanism behind the remarkably high IRI activity of PVA has eluded researchers. This study aims to determine effect of dispersity on IRI activity of low molecular weight PVA and define the chain length where IRI activity of PVA deviates from other poly-ols.

Short chains of poly(vinyl acetate) (PVAc) were synthesised by reverse addition/fragmentation transfer (RAFT) polymerisation. This was followed by purification *via* column chromatography, yielding ultra-low dispersity PVAc oligomers that were subsequently deprotected to PVA.

IRI investigations revealed that more disperse PVA samples are more active than the ultra-low dispersity oligomers. 5 repeat unit increases in chain length were found to increase IRI activity. Comparisons between poly-ols and short chain PVA found PVA with a chain length of 12.5 is more active than poly-ols with a similar degree of hydroxylation, providing evidence of IRI activity in PVA activating at this chain length.

<u>Acknowledgements</u>

Contents

Figures

Abbreviations

Đ	M_w/M_n
ACVA	4,4' azobis(4-cyanovaleric acid)
AF(G)P	Antifreeze(glyco) protein
CRP	Controlled radical polymerisation
CTA	Chain transfer agent
DIS	Dynamic ice shaping
DP	Degree of Polymerisation
ESI	Electrospray ionisation
HES	Hydroxy ethyl starch
IR	Infrared
IRI	Ice recrystallisation inhibition
LC	Liquid chromatography
TH	Thermal Hysteresis
MADIX	Macromolecular Design via the interchange of Xanthates
mg	Milligram
MGS	Mean grain size
mL	Millilitre
MLGS	Mean largest grain size
M_n	Number average molecular weight
MS	Mass spectrometry
M_w	Weight average molecular weight
NMR	Nuclear magnetic resonance spectroscopy
PBS	Phosphate buffered saline
PiPA	Poly(isopropenyl alcohol)
PVA	Poly(vinyl alcohol)
PVAc	Poly(vinyl acetate)
PVP	Poly (vinyl pyrolidone)
RAFT	Reverse Addition/Fragmentation Chain Transfer
R_f	Retardation factor
SEC	Size exclusion chromatography
TLC	Thin layer chromatography
THF	Tetrahydrofuran

1. Introduction

1.1. Antifreeze(glyco) proteins

The fact that fish can survive in the arctic seas is a curious one. Temperatures in polar seas hover around the freezing point of seawater (-1.8 °C). This temperature implies that, ice crystal formation in blood should be an issue for fish in these areas. To combat this, blood plasma in polar fish contains a high concentration of dissolved sugars and salts and a specialised series of glycoprotein termed antifreeze(glyco) proteins (AF(G)P). Originally isolated by Devries,[1] these proteins are based on a highly conserved alanine-alanine-threonine sequence with a disaccharide at the threonine residue (*Figure 1.*).[2]

Figure 1. Structure of AF(G)P found in arctic fish

The mechanism of action of AF(G)Ps in water is a matter of debate. Recently, Meckerell and co-workers have used molecular dynamics simulations to suggest that AF(G)Ps perturb long range water dynamics.[3] They proposed that the conformation of the carbohydrate moiety on the AF(G)P allows the hydroxyl groups to form stable water bridges. These bridges influence the hydrogen-bond network in water, and disrupt the tetrahedral network of water molecules up to 20 Å away from the AF(G)P itself. While these latest findings are fascinating, a full picture of the AF(G)P antifreeze mechanism remains elusive.

The potential applications for antifreeze proteins are widespread: from reducing freezer burn in frozen foods to lowering the risk of ice formation damaging to airplane components.[4–6] An important application lies in cryopreservation, specifically in the areas of regenerative and transplantation medicine. Preservation of donated blood simply by freezing results in the puncturing of red blood cells by ice crystals; similar problems are encountered when preserving organs. With high demand for donated blood in hospitals and successful organ transplants needing perfect tissue preservation; there is a need for novel cryopreservation techniques that preserve cells and tissues without damaging them. At the moment, AF(G)Ps in isolation have not found many successful applications in cryobiology, as reviewed by Duman;[7] but their potential to be used in combination with other nature inspired strategies is an open question.

1.2. Definition of 'antifreeze'

Gibson reviewed the potential of synthetic mimetics of AF(G)Ps as cryoprotectants.[8] Central to this work was a detailed examination of what constitutes antifreeze activity. Antifreeze activity can be separated into three separate processes: thermal hysteresis (TH), dynamic ice shaping (DIS) and ice recrystallisation inhibition (IRI).

TH is effectively a freezing point depression. A solution containing AF(G)P will have a freezing point that is lower than its melting point, the corresponding gap is referred to as the TH gap. Holding an ice crystal isothermally within the TH gap of an AF(G)P solution will result in no crystal growth until the temperature is moved out of the range of the TH gap. Determining this gap is usually done through using a nanolitre osmometer to observe the growth of a single ice crystal.[9]

DIS is the ability of a solution containing antifreeze to alter the morphology or crystal habit of an ice crystal. Typically the morphology of an ice crystal is determined near its freezing point, or within the TH gap if there is one. In the presence of AF(G)Ps, ice adopts hexagonal structures. As the AF(G)P concentration is increased, hexagonal bipyramidal structures are seen (*Figure 2.*).[10]

The third property, and most important for cryopreservation, is IRI. IRI refers to the inhibition of the rate of growth of ice crystals. It is distinct from the ability to depress the freezing point and supress ice nucleation. Ice recrystallisation occurs when larger ice crystals grow at the expense of smaller ones. This is due to an Otswald ripening process making it more favourable for larger ice crystals to exist.[11] On larger ice crystals there is smaller proportion of surface water molecules with energetically unfavourable dangling bonds. Water molecules on the surface of smaller ice crystals tend to detach, following the Kelvin equation, and deposit onto larger crystals.[11] This leads to preferential formation of larger ice crystals, classically seen in ice cream that has been kept frozen for a long time. IRI hinders the ability of ice crystals to grow in this manner and results in the ice crystals in an AF(G)P solution remaining small. A molecule with high IRI activity will therefore produce small ice crystals when frozen in solution.
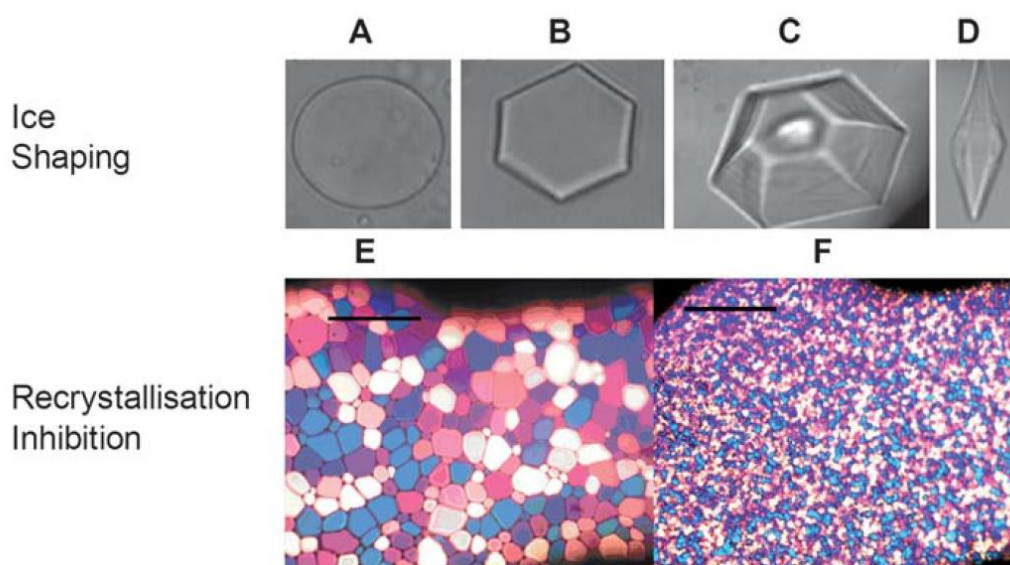
Figure 2. Observation of thermal hysteresis and recrystallisation inhibition activity using optical assays, single ice crystals on freezing stage of a microscope (A) no inhibitors; (B) dilute solution of AFP; (C) "step pinning" causing ridges to appear in ice crystals; (D) High concentration of AF(G)P causing hexagonal bpyrimadal ice crytals (E) and (F) asssays showing recrystallisation inhibition. Phosphate buffered saline solution prepared using ''splat'' assay after 30 minutes: (E) no additives; (F) with 5 mg mL^{-1} poly(vinyl alcohol)$_{2625}$.[8]

1.3. Synthetic mimetics of AF(G)Ps

1.3.1 Poly(vinyl alcohol)

Gibson's review established the potential for synthetic mimetics of AF(G)Ps as possible cryoprotectants.[8] Primarily, the review focussed on polymers as synthetic mimetics of AF(G)Ps in preference to peptides/ proteins. This is due to the relatively straightforward nature of polymer synthesis compared to protein synthesis, and the relative ease at which polymer properties and functionality can be manipulated.

Antifreeze properties have been indicated in several classes of synthetic polymer,[8] this alone is a surprising result. It would seem logical that the antifreeze activity of AF(G)Ps is due to their unique three dimensional structure. The fact that it can be found in far more poorly defined synthetic polymers is a surprise in itself, deepening the mystery regarding the IRI mechanism. The most remarkable result of all is the identity of the most active antifreeze polymer: poly(vinyl alcohol) (PVA) (*Figure 3.*).
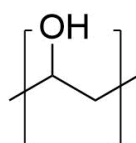
Figure 3. Chemical structure of poly(vinyl alcohol).

Knight *et al.* first reported the anomalously high IRI activity of PVA.[12] The authors had no explanation for the antifreeze activity of PVA, it was assumed that the unique three dimensional structure of AF(G)Ps was fundamental to their antifreeze capability. Crucially, PVA does not cause TH or DIS – its only antifreeze property is IRI.[13] This has implications for cryopreservation as needle shaped ice formed by DIS damages cells during thawing, IRI only prevents ice crystal growth.[14]

The Gibson group, and others, have carried out extensive studies into the IRI activity of PVA.[15–19] Deller *et al.* compared the IRI activity of carbohydrate based poly-ols with PVA.[17] It was found that the molecular weight (MW) of the carbohydrate based poly-ols had no impact on their IRI activity (*Figure 4.A.*); in contrast, the IRI activity of PVA is heavily dependent on MW. Higher MW PVA is more IRI active (*Figure 4.B.*). Therefore the IRI mechanism of PVA can be reasonably assumed to be different to poly-ols. In this study the role of hydrophobic domains was also probed, establishing that PVA in solution presents a hydrophobic domain without self-aggregation - it was hypothesized that this plays a key role in the IRI activity of PVA.
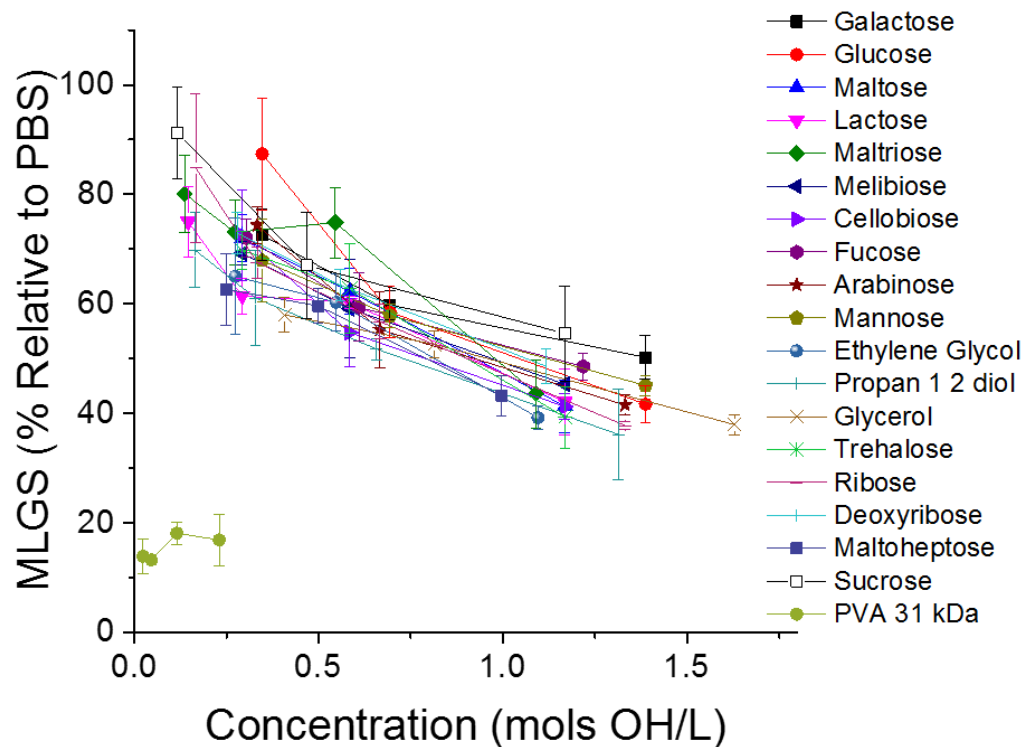
Figure. 4 A. IRI activity of poly-ols compared to PVA (MLGS = mean largest grain size; lower MLGS equates to higher IRI activity).[20]
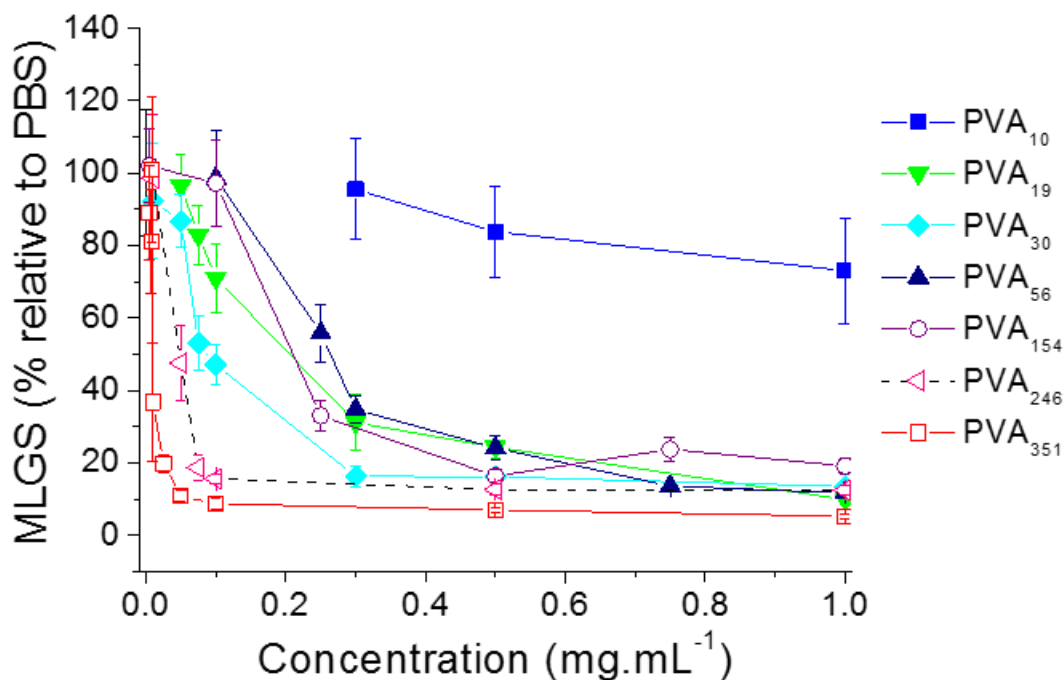
Figure. 4 B. The dependence of IRI activity on MW of PVA (MLGS = mean largest grain size; lower MLGS equates to higher IRI activity).[16]

To further probe the IRI mechanism, Congdon *et al.* studied the structure-activity relationship of PVA and IRI.[16] Rigorously defined PVA accessed by Reverse Addition/Fragmentation Chain Transfer (RAFT) polymerisation was used. In contrast, earlier studies used commercial samples of PVA that were highly disperse and partially acetylated.[15,21] These characteristics mean commercial PVA is unsuitable for reliable structure – activity relationship studies of PVA and IRI. Using well defined polymers from RAFT polymerisation established a 'switching on' of IRI activity in PVA between degree of polymerisation (DP) 10 and DP 19. The study also explored structural modifications to PVA (*Figure 5.*). Addition of hydrophobic acetyl groups to PVA lead to a reduction in IRI activity. Logically, the group then examined the effect of addition of hydrophilic PVP groups to PVA and saw a similar loss of IRI activity – though up to 20 % PVP was tolerated with small IRI activity loss. These two results provide the interesting observation that addition of either hydrophobic or hydrophilic groups to PVA lowers its IRI activity. Therefore, neither of these properties in isolation accounts for IRI activity. The block copolymer, PVA-*co*-PiPA, was synthesised to test whether the spacing of hydroxyl groups was a key influence on IRI activity, as this copolymer maintains the hydroxyl group spacing of PVA with the addition of a pendant methyl group. PVA-*co*-PiPA was IRI active but was still less active than PVA, showing the addition of hydrophobic units to the main chain does not increase the IRI activity of PVA, leading to

the idea that the conformation of PVA in solution is key to its unique IRI activity and any modifications to this conformation lead to a reduction in activity.
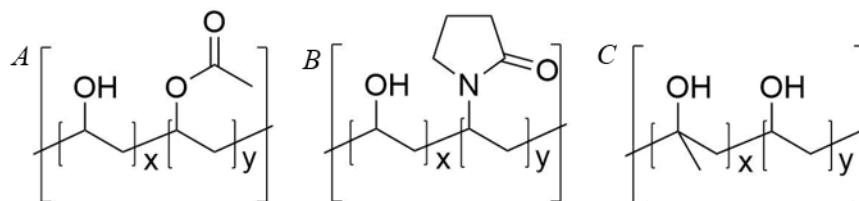
Figure 5. (A) partially acetylated PVA, (B) PVA-co-PVP, (C) PVA-co-PiPa.

In the above discussion, the copolymers investigated were randomly distributed throughout the polymer chain. Congdon *et al.* then investigated the influence of block copolymers on the IRI activity of PVA.[19] Addition of large hydrophobic block copolymers had no effect on the IRI activity of PVA, giving further evidence that the unbroken chain of hydroxyl groups is important in the IRI mechanism. This work provided the first examples of structural modifications of PVA not influencing the IRI activity. Congdon and Philips have also demonstrated use of an Fe based supramolecular trigger to switch on PVA IRI activity.[22]

One of the ultimate goals in investigating the IRI activity of PVA is its applications in cryopreservation. Deller *et al.* have demonstrated that PVA enables non-vitreous cryopreservation of cells by reducing ice crystal growth during thawing.[23] A mere 0.1 weight % PVA was required to increase cell recovery, in contrast to the 20 weight % required from conventional solvent based strategies. Combinations of PVA and the polymeric cryoprotectant hydroxyl ethyl starch (HES) have also been employed by Deller, leading to increased cell recovery compared to pure PVA.[24] Gibson and co-workers have also shown that shorter polymers are more effective for cellular cryopreservation, as high MW PVA lead to greater DIS. [20]

To conclude, PVA is highly IRI active and all modifications made to its structure so far have resulted in decreased or equal IRI activity. The IRI mechanism remains shrouded in mystery, specifically the 'switching on' of IRI activity between DP 10 and DP 19. Selected other IRI active species under investigation will be briefly reviewed here.

1.3.2. Poly(ampholytes)

In pursuit of a rationally designed polymer with IRI properties, Gibson and co-workers have synthesised poly(ampholytes).[25,26] Poly(ampholytes) are IRI polymeric species with both cationic and ionic side chains. As with PVA, their mode of action regarding IRI is unclear. Poly(ampholytes) are less IRI active than PVA, but still demonstrate cell

recovery of up to 60 %.[25] Investigations into the effect of back bone and side chain hydrophobicity found that side chain hydrophobicity has a significant impact on IRI activity. [26] Increased side chain hydrophobicity of up to 10 mol % increased IRI activity, beyond this the effect diminished: leading to the conclusion that simply increasing hydrophobicity does not increase IRI activity. This was the first report of a tuneable polymer demonstrating IRI activity, though it was still not as active as PVA.

Matsumura and Hyon have also investigated cryopreservation with poly(ampholytes). A carboxylated poly-l-lysine (>50 % amino acids carboxylated) was found to give a 95 % recovery post thawing of murine L929 cells.[27] In an attempt to elucidate the mechanism of cryoprotection of cells, Matsumura synthesised further poly(ampholytes).[28] Increased hydrophobic character in poly(ampholytes) resulted in better affinity for the cell membrane.

1.3.3 Small Molecule AF(G)P Mimetics

The group of Ben has been investigating the potential for small molecule peptide based mimetics of AF(G)Ps.[29] The group has synthesized a series of small molecules based on the structure of AF(G)Ps. They have found mono- and disaccharide variants that demonstrate IRI activity approaching that of native AF(G)P, with a galactose monosaccharide the highlight (*Figure 6.*). [30] IRI activity investigations of this molecule gave a mean average largest grain size (MLGS) of 20 % compared to the phosphate buffered saline (PBS) control. In contrast, PVA with DP > 19 gives an MLGS of 14 % of the PBS control. Capiciotti *et al.* have also investigated *O*-aryl-glycosides as cryoprotectants. Mean grain size (MGS) values of up to 10 % PBS have been achieved when the R group was a halogen. [31,32]
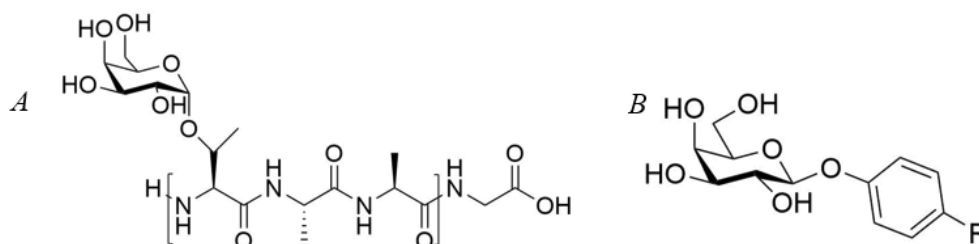
Figure 6. IRI active small molecules: (A) galactose AF(G)P mimic. (B) O-aryl glycoside

1.4 Chain length dependence and the effect of dispersity on IRI
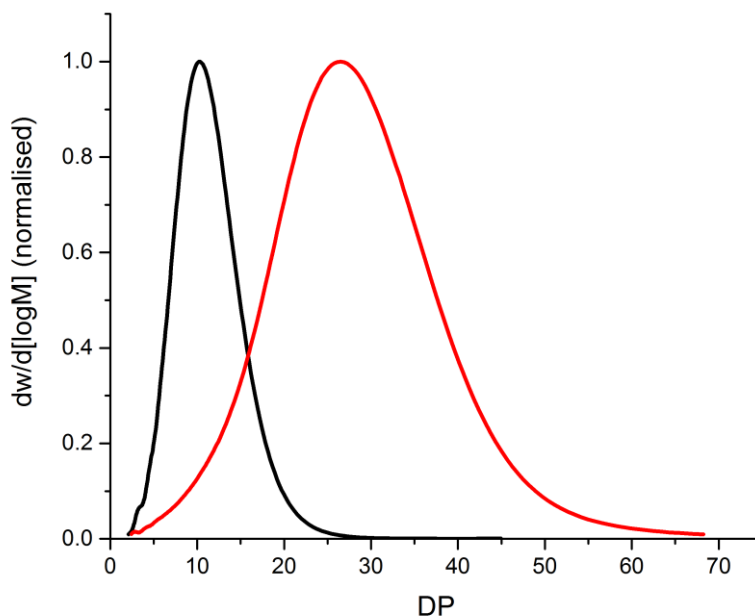
Figure 7. Distribution of chain lengths in the DP 10 and DP 19 polymers tested by Congdon et al.

As discussed above, Congdon reported IRI activity in PVA activates between DP 10 and DP 19.[16] The polymers used to determine this had a dispersity (Đ) of 1.18, with a relatively broad distribution of chain lengths (*Figure 7.*). PVA_{19} was more active than PVA_{10} but, due to the chain length distribution, the minimum chain length for IRI activity is still unknown. Very low dispersity is required to obtain a more accurate minimum chain length, methods to access low dispersity polymers are now considered.

1.4.1 Dispersity

All polymers are disperse.[33] Polymer samples are composed of a variety of chain lengths, so the chain length of a sample (given by DP) is only an approximate value. Dispersity is a mathematical expression of the distribution of chain lengths and is given by the ratio of the weight average molecular weight and the number average molecular weight (equations 1 – 3).

$$M_n = \frac{\sum N_i M_i}{\sum N_i} \tag{1}$$

$$M_w = \frac{\sum (N_i M_i^2)}{\sum (N_i M_i)} \tag{2}$$

$$Đ = \frac{M_w}{M_n} \tag{3}$$

To illustrate the effect of dispersity: a DP 8 polymer with Đ=1.2 might only have 15 % of its chains actually 8 repeat units long, while also having chains as small as 3 repeat units and as large as 12 repeat units. This demonstrates the complexity inherent in homopolymers. Polymers with low dispersity are often a synthetic target, as well defined polymers usually have more consistent properties than highly disperse variants. Typically, dispersity is measured by size exclusion chromatography (SEC) but can also be measured by mass spectrometry (MS). [34,35]

1.4.2 Strategies for obtaining low dispersity polymers

Classically, low dispersity polymers are obtained by living polymerisation. Living polymerisation is a form of radical polymerisation where no termination occurs and the chain continues to grow until it runs out of monomer. The lack of termination in these reactions results in very low dispersity. In practice, the conditions these polymerisations require (typically low temperatures and argon atmospheres) means it is usually more convenient to do controlled radical polymerisation (CRP) to obtain similar results.

Currently, RAFT or Macromolecular Design *via* the interchange of Xanthates (MADIX) polymerisation is often the CRP method used to obtain low dispersity PVA, as it is particularly effective for vinyl monomers.[36] Dispersity control in RAFT polymerisation originates from the equilibrium between growing radical chains and dormant chains, causing all chains to grow at the same rate (*Scheme 1. (4)*). Destarc has extensively reviewed polymerisation of vinyl ester compounds via RAFT.[36] Through careful selection of R and Z groups, Đ ≈ 1.1 can be accessed.
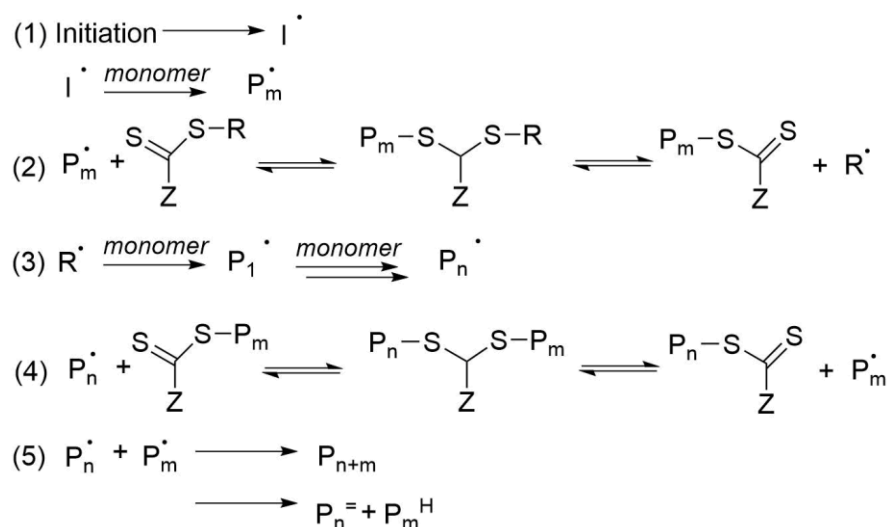
Scheme 1. Mechanism of RAFT/ MADIX Polymerisation.[37]

Accessing Đ < 1.1 can be challenging. Reports of polymers with Đ < 1.1, the techniques used to access them, the relevant monomers and their MW limitations are summarised here (*Table 1.*). It is clear that the column chromatography approach by Hawker *et al* provides polymers with the lowest dispersity in the very short chain length regions this study is concerned with.[38] Hawker obtained discrete (Đ = 1) oligomers in the region of DP 3 to DP 13 on a gram scale by doing flash chromatography on short (DP ~8) polymers obtained by CRP. Hawker's approach is limited to short, oligomeric materials; with Đ > 1 seen when DP > 14.

Method	Monomer	Đ[a]	M_n	Author(s)
Aqueous RAFT		1.06	13900	Martin *et al.*[39]
RAFT		1.04	14400	Chiefari *et al.*[40]
SET LRP		1.08	10,500	Haddleton *et al.*[41]
Low temperature RAFT		1.08	117500	Wiggins *et al.*[42]
Column Chromatography		1		Hawker *et al.*[38]
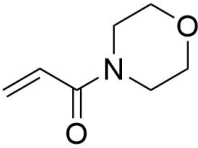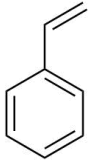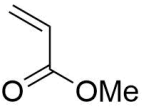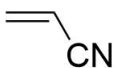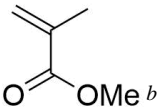
Table 1. Techniques and relevant monomers used to access low dispersity polymers. [a] Đ=Mw/Mn ,[b]example monomer

The other strategies outlined do present examples of remarkable dispersity control at high MW. However, the convenience and simplicity of Hawkers approach makes it the ideal strategy for this study.

Other approaches to low dispersity polymers through chromatography have been reported; for example SEC, TLC and LC.[35,43,44] These approaches tend to produce analytical scale quantities of reagents and are limited by loading capacity and resolution. To the author's knowledge, Hawker's column chromatography approach is the only report of synthetically useful yields of discrete oligomers by separation.

Obtaining a series of monodisperse PVA will enable a detailed investigation of the 'switch on' region of IRI activity, deepening understanding of structure-activity relationship between PVA and IRI. Mechanistic understanding of IRI is essential to facilitate the rational design of novel cryopreservatives that can preserve frozen tissue without damaging it.

1.5 Project Aims

With the IRI mechanism of PVA still unknown, this project will investigate the 'switch on' region of IRI activity of PVA between DP 10 and DP 19.

i) Poly(vinyl acetate) (PVAc) between DP 10 and DP 19 will be synthesised by RAFT polymerisation and then separated by column chromatography with the goal of obtaining monodisperse oligomers of PVAc. These will then be deprotected to PVA.

ii) The chain length that "switches on" IRI activity will be investigated by testing the IRI properties of these oligomers.

iii) The IRI activity of PVA oligomers will be compared to the IRI activity of poly-ols containing a similar number of OH groups to determine when PVA IRI activity deviates from that of poly-ol materials.

2. Results and Discussion

2.1 Synthesis of PVA Oligomers with ultra-low dispersity

2.1.1 Chain Transfer Agent Synthesis

Direct polymerisation of vinyl alcohol is not possible due to vinyl alcohol existing as its more stable tautomer acetaldehyde. Therefore, it is necessary to polymerize vinyl acetate followed by deprotection of the acetate groups. To reduce the starting dispersity relative to free radical polymerization, for subsequent purification, RAFT polymerisation was employed. This required the synthesis of a chain transfer agent (CTA). Previous work in the group had shown that vinyl acetate polymerises efficiently with methyl (ethoxy carbonthioyl) sulfanyl acetate (CTA 1). A literature method was followed.[22] In short, carbon disulphide was reacted with ethanol/ KOH, followed by nucleophilic attack on methyl bromoacetate, resulting in 39 % yield after purification. Satisfactory characterisation data was obtained (*Figure 8.*)
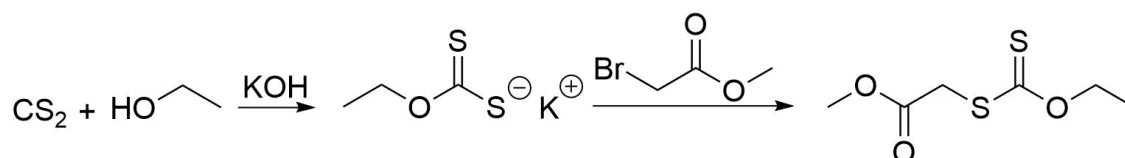
Scheme 2. Synthesis of CTA 1.
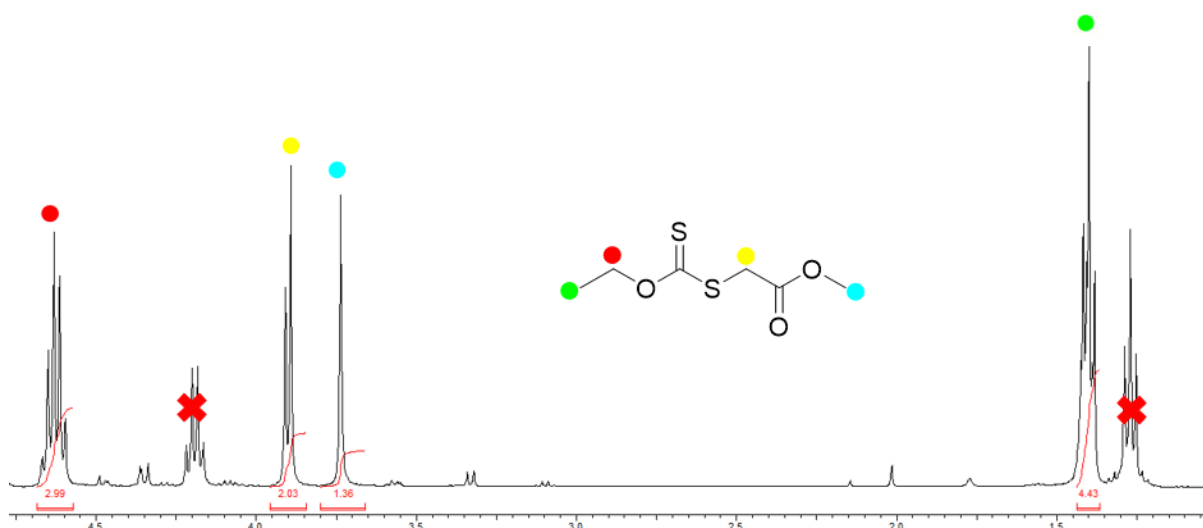
Figure 8. ^{1}H NMR of CTA 1, red crosses indicate ethanol.

2.1.2 PVAc synthesis

PVAc was synthesised by polymerisation of vinyl acetate with CTA 1 and initiated by 4,4' azobis(4-cyanovaleric acid) (ACVA) under an inert atmosphere (*Scheme 3.*). Use of solvent reduces monomer concentration and slows the propagation of the reactions. Therefore, the polymerisations were carried out in bulk. Following the reaction, polymers were obtained by precipitation in hexane. To confirm we could access polymers of the desired MW range, a series of test polymerisations with a range of monomer-CTA ratios from 50 to 200 were conducted (*Table 2.*). Manipulation of the monomer to CTA ratio allowed access to DP from 50 to 200. Theoretical DP and DP obtained by experimental analysis (SEC and ^{1}H NMR) were generally well aligned.
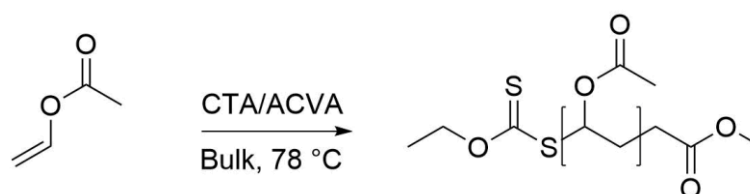
Scheme 3. CTA 1 mediated polymerisation of vinyl acetate to yield poly(vinyl acetate).

Polymer	[M]/[CTA]^a	DP$_{theo}$^{b}	DP$_{NMR}$^{c}	DP$_{sec}$^{d}	M$_{n,sec}$^{e} (g/ mol)	M$_{w,sec}$^{f} (g/ mol)	Đ$_{sec}$^{g}
PVAc$_{15}$	15	15	26	21	1800	2200	1.23
PVAc$_{50}$	50	50	66	44	3800	5100	1.34
PVAc$_{75}$	75	75	117	89	10200	12500	1.32
PVAc$_{100}$	100	100	100	100	8600	12200	1.42
PVAc$_{125}$	125	125	159	115	9900	13400	1.36
PVAc$_{150}$	150	150	182	172	14800	24500	1.65

Table 2. ^{a}Monomer to RAFT agent ratio. ^{b}Theoretical DP determined to monomer to RAFT agent ratio. ^{c}Degree of of polymerisation determined by ^{1}H NMR. ^{d}Degree of polymerisation determined by SEC. ^{e}Number average molecular weight determined by SEC. ^{g}Weight average molecular weight determined by SEC. ^{h}M$_w$/M$_{n..}$

Hawkers technique for obtaining monodisperse oligomers by column chromatography was done with low dispersity, low MW polymers.[38] Therefore, low dispersity PVAc in the region of DP 10 – 20 was needed before further purification could take place. Initially a monomer-CTA ratio of 15 was investigated (*Table 2, PVAc₁₅*). A higher than expected DP was observed. A trend of higher than expected DP was seen in all attempts to polymerise low DP PVAc (*Tables 2., 3. and 4.).* The poor control over the reaction is likely due to the large difference in reactivity between the growing chain (high) and the monomer (low),[36] this reactivity difference increases the propensity of side reactions such as chain transfer to monomer and polymer, leading to poor control over the MW distribution.[45] The formation of oligomers by RAFT is also complicated by the initial free-radical polymerization before the RAFT equilibration is established, leading to poorer MW control.[45] Also, in low molecular weight polymers, DP measurements by SEC have a tendency to overestimate,[46] which could also be a factor in the unexpectedly high DP observed.

2.1.3 The feasibility of separating PVAc by column chromatography

With the goal of producing PVA oligomers, testing of the feasibility of separating PVAc by column chromatography was conducted. Initially, target DP 10 PVAc was synthesised. This DP was chosen as it is in the 'switch on' region of IRI activity as reported by Congdon[16] and similar chain lengths were separated by Hawker in his report of discrete oligomers by column chromatography.[38]

Polymer	[M]/[CTA]^a	DP$_{theo}$^{b}	DP$_{NMR}$^{c}	DP$_{sec}$^{d}	M$_{n,sec}$^{e} (g/ mol)	M$_{w,sec}$^{f} (g/ mol)	Đ$_{sec}$^{g}
PVAc$_{16}$	10	10	13	19	1700	1900	1.01

Table 3. ^{a}Monomer to RAFT agent ratio. ^{b}Theoretical DP determined to monomer to RAFT agent ratio. ^{c}Degree of of polymerisation determined by ^{1}H NMR. ^{d}Degree of polymerisation determined by SEC. ^{e}Number average molecular weight determined by SEC. ^{f}Weighted average molecular weight determined by SEC. ^{g}M$_w$/M$_n$.

Firstly, an appropriate solvent system was refined. Investigations were carried out by thin layer chromatography (TLC) of PVAc₁₆. The intent was to 'smear' the sample across the whole plate, with low MW chains at the top and high MW chains at the bottom. Taking fractions by column chromatography would then correspond to low dispersity 'slices' of the whole polymer sample (*Figure 9.*). It was found that a 75:25 ratio hexane-ethyl acetate provided appropriate separation of PVAc₁₆.
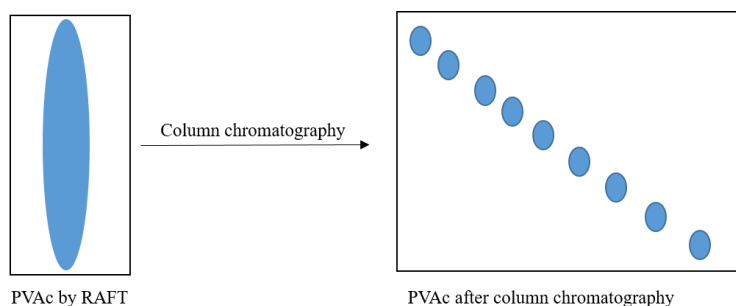
Figure 9. Cartoon of TLC plate of PVAc with desired separation and separation of fractions after column chromatography

Having established a solvent system, investigations into fractionating PVAc by column chromatography were conducted. 0.4 g of $PVAc_{16}$ was loaded onto a silica column and separated using flash chromatography with a 75:25 ratio of hexane-ethyl acetate solvent. In this initial experiment, 14 fractions were taken. TLC analysis was carried out to see if separation was taking place (*Figure 10.*). The TLC plates were encouraging. The linear decrease in retardation factor (R_F) values with increased fraction number implied that separation by chain length had occurred. The fractions were then dried *in vacuo.* Yields from the individual fractions were in the region of 1 – 10 mg. SEC analysis was carried out, demonstrating an inverse relationship between fraction number and retention time (representative data, *Figure 11.*). This indicated that separation by MW had been successful and that the PVAc could be fractionated by simple column chromatography.
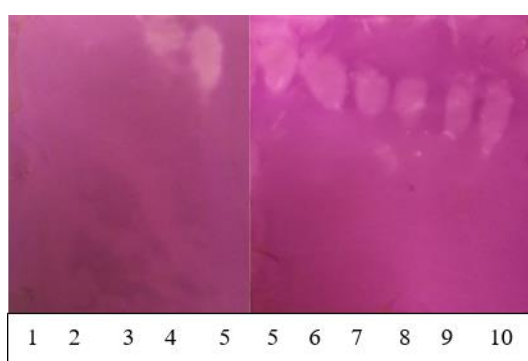
Figure 10. TLC plates demonstrating the feasibility of separating PVAc by column chromatography.
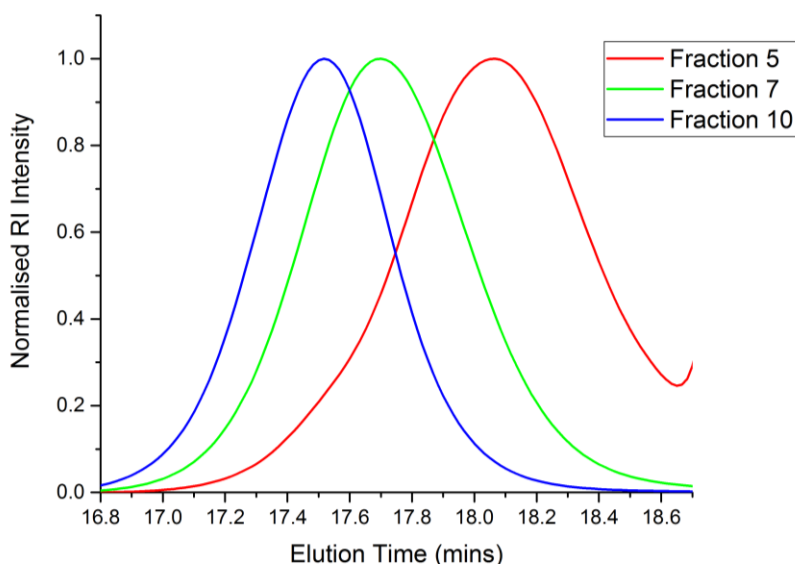
Figure 11. THF SEC traces for PVAc separated by column chromatography.

While SEC gave evidence that the fractions had separated by retention time, other data provided by SEC (M_n, Đ) did not correlate to our expectations. This is likely due to the difference in hydrodynamic volume of PVAc *vs*. the calibrants used in the SEC: (poly(styrene) and poly(methyl methacrylate) and the broad MW range the SEC is calibrated to work over. For this reason, we turned to mass spectrometry (MS) for characterisation of the separated polymers, as MS has been demonstrated to provide more accurate data for low MW, low dispersity polymers.[47] For convenience, electrospray ionisation (ESI) MS was used due to the ease of sample preparation and previous work in the group finding that PVAc is well suited to analysis by ESI-MS.

The mass spectra of the fractions (*Figure 12.2-12.9.*) have a noticeably smaller distribution of chain lengths than the mass spectrum of the original polymer *(12.1)*. An increase in molecular weight with increased fraction number is also visible, with the fractions covering the full molecular weight range of the original polymer. Lower MW fractions generally had a narrower dispersity than the higher MW fractions. Fraction *12.2* was particularly exciting due to the very low distribution of chain lengths. Better separation in the lower MW fractions was expected due to the nature of separation by polarity. The relative differences in polarity between a DP 3 and a DP 4 PVAc chain is significantly larger than the relative polarity difference between a DP 13 and DP 14 chain. Therefore, the shorter chain were better resolved by column chromatography as the difference in affinity for the stationary phase (silica gel) is larger between shorter chain lengths than it is for larger chain lengths.
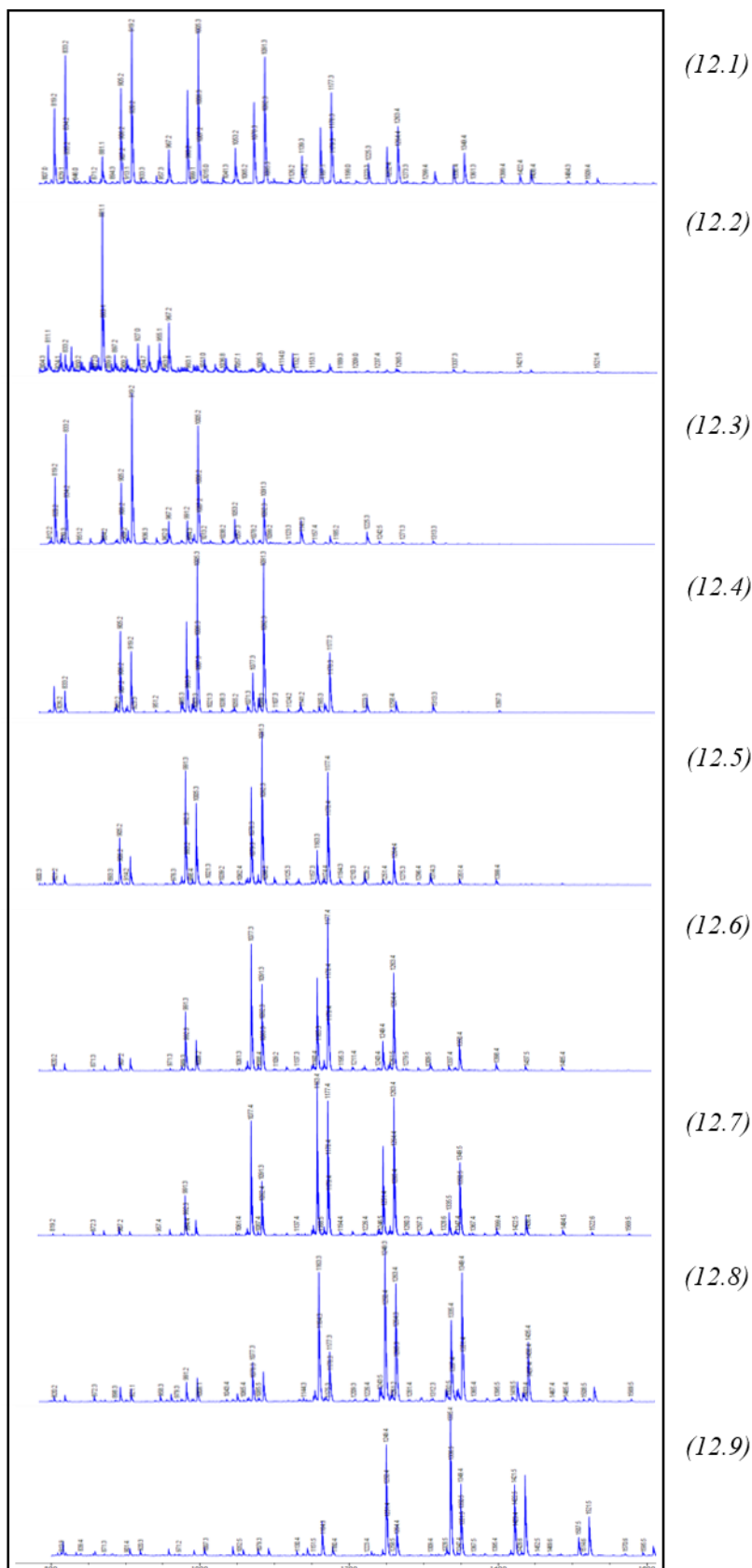
Figure 12. ESI-Mass spectra of PVAc$_{16}$ (12.1) and of PVAc obtained by separation of PVAc$_{16}$ by column chromatography (12.2-12.9)

2.1.4 Large scale separation of PVAc by column chromatography

The above data confirmed that, in principle, it is possible to separate low MW PVAc by column chromatography. Encouraged by this, PVAc samples in the region of DP 5 - 13 were sythesised on a 10 g scale in an attempt to obtain fractions from the column that yielded massses of PVAc suitable for conversion to PVA for IRI testing.

Polymer	[M]/[CTA][a]	DP_{theo}[b]	DP_{NMR}[c]	DP_{sec}[d]	Mn_{sec}[e] (g/mol)	Mw_{sec}[f] (g/mol)	$Đ_{sec}$[g]
$PVAc_6$	6	6	5	12	1050	1080	1.03
$PVAc_{10}$	10	10	17	14	1240	1420	1.14
$PVAc_{13}$	13	13	16	19	1600	1740	1.08

Table 4. [a]Monomer to RAFT agent ratio. [b]Theoretical DP determined to monomer to RAFT agent ratio. [c]Degree of of polymerisation determined by ^{1}H NMR. [d]Degree of polymerisation determined by SEC.[e]Number average molecular weight determined by SEC. [f]Weighted average molecular weight determined by SEC. [g]M_w/M_n.

An appropriate solvent system was refined for each separate PVAc sample using the same TLC strategy as described above. Each polymer was then loaded onto a column and separated by flash chromatography. The separation was once again tracked by TLC *(Figure 13.)*. Approximately 80 fractions were obtained for each separation, the columns were stopped when no separation was visible by TLC. Each fraction was analysed by mass spectrometry. Generally, a yield of 50 – 100 mg of PVAc was obtained in each fraction.
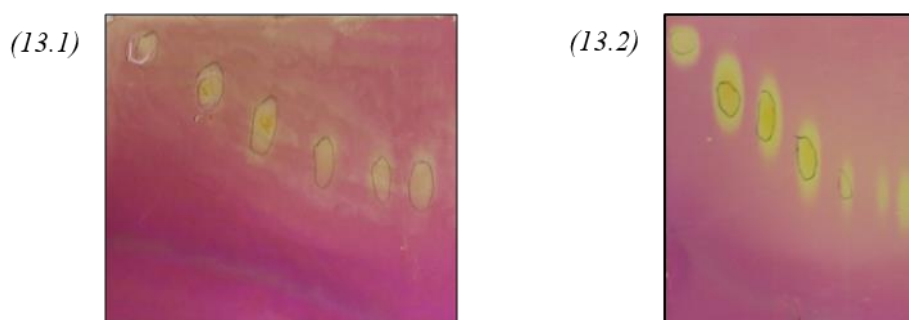
Figure 13. TLC plates of separation of (13.1) PVA$_{10}$ (13.2) PVA$_{13}$

Interestingly, separation of PVAc$_6$ enabled resolution of individual chain lengths by TLC (*Figure 14.*). Clearly, at these short chain lengths, the relative differences in polarity between different PVAc chain lengths are enough large to enable resolution at the single chain length level.

Figure 14. Individual chain length resolution of PVAc$_6$ by TLC.

In general, shorter chain lengths were better resolved by this approach than longer chain lengths. This is expected due to the relative polarity difference between two short chains being larger than the relative polarity difference between two longer chains. The best resolution was obtained between DP 5 and DP 14, fractions above this contained a significantly broader mix of chain lengths.

At this point, the limitations of using dispersity as a means to describe the distribution of chain lengths in low MW polymers became clear. Dispersity is biased towards higher chain lengths. For example, a hypothetical polymer with two chains of DP 1000 and 1001 would have a dispersity of 1.001. In contrast, a polymer chain length of 11 and 10 would have a dispersity of 1.1. The difference in DP in the two polymer samples is exactly the same, but one has a dispersity two orders of magnitude lower than the other. In our case, dispersity values for the very low MW samples in this investigation made the polymers look more disperse than they actually were. *Figure 15* shows mass spectra of two different PVAc samples, the higher MW sample (*Figure 15.1*) clearly has a broader distribution of chain lengths than the other. But the higher MW of *15.1* results in it having a lower dispersity, despite it having a broader distribution of chain lengths.
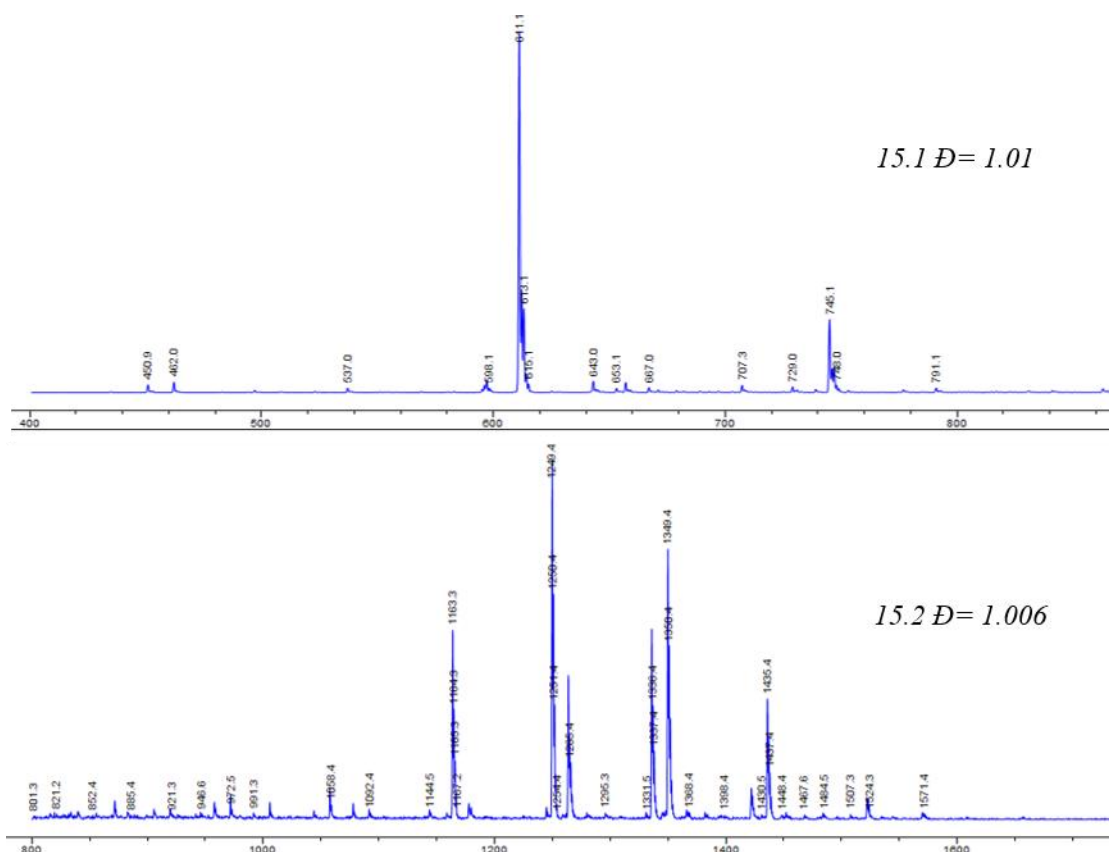
Figure 15. ESI-MS for comparison of Đ for PVAc samples of different MW.

With the limitations of dispersity as a useful means of comparison of oligomers established, there was a need to devise a method to easily compare both the range of chain lengths in a sample and the amount of each chain length. While MS provides all of this information; it is not presented in a digestible form due the variety of fragment ions seen in the mass spectrum. For example: the end groups from the CTA could be present in their entirety, or only the α or ω groups, or there could be a combination of end groups and common ions such as potassium or sodium. Water and methanol are also commonly seen adducts in ESI-MS.[48] A representative example of a fully assigned PVAc mass spectrum is shown below (*Figure 16*).
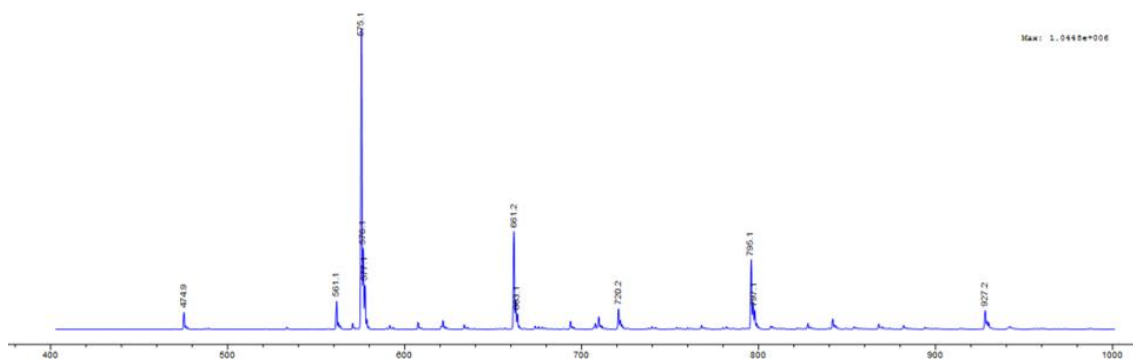
m/z 474.9 (10%, α-$(CH_2CH(CO_2Me))_3$-ωNa^+), 561.1 (12, α-$(CH_2CH(CO_2Me))_4$-ωNa^+), 575.1 (100, $(CH_2CH(CO_2Me))_5$-ωNa^+), 661.2 (28, $(CH_2CH(CO_2Me))_6$-ωNa^+), 720.2 (12, $(CH_2CH(CO_2Me))_7$-ω), 795.1 (22, α-$(CH_2CH(CO_2Me))_7$-ω), 927.2 (8, $(CH_2CH(CO_2Me))_7$-ω MeOH)

Figure 16. Fully assigned ESI MS of a PVAc sample.

To facilitate easy comparison of polymer samples the following graphical representation of MS data was devised. The data was generated by fully the mass spectra of each fraction. Next, the weight of each peak was obtained as fraction of the tallest peak. The weightings of each peak were grouped by DP and plotted on the following graphs (representative data: *Figure 17*). These graphs facilitate easy and accurate comparison of chain length distribution between polymer samples, without being affected by the MW bias inherent when using dispersity as a measure.
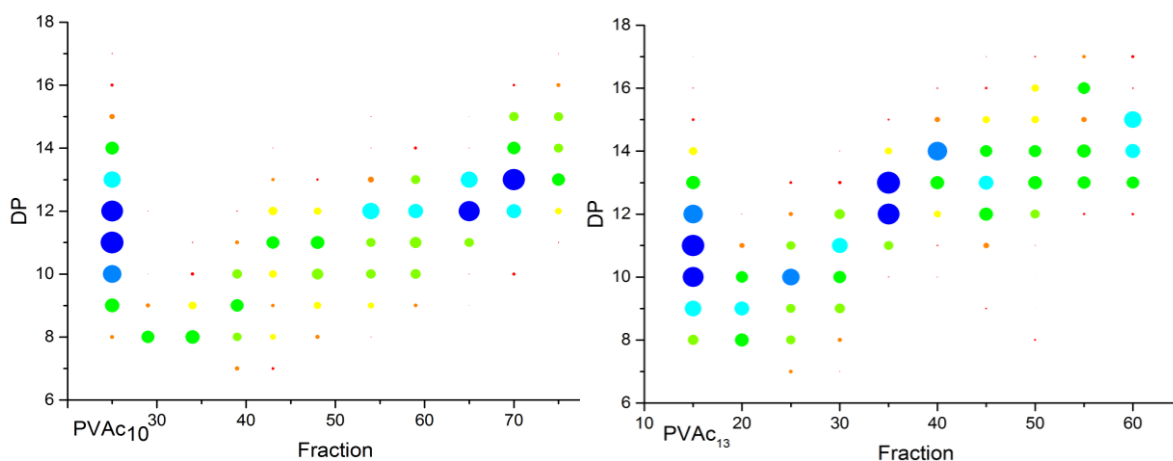
Figure 17. Graphical representation of the distribution of chain lengths within separated samples of PVAc$_{10}$ and PVAc$_{13}$. Chain length distributions of the original, unseparated polymers are shown on the left of each graph to demonstrate extent of separation.

These graphs further demonstrate characteristics of PVAc separated by column chromatography. As expected, the lowest chain length distribution is seen for shorter chain lengths (DP 5, 6 and 7). Above DP 12, broader distributions of chain lengths are seen, this also aligns with the work of Hawker who obtained mixtures of chain lengths above DP 13.[38] No truly monodisperse samples were obtained with this approach but, to the authors' knowledge, separation of PVAc by column chromatography provides access to narrower chain length distributions at these very low chain lengths than any CRP techniques. Having obtained this data, finding the lowest dispersity PVAc was straight forward. The final library of ultra-low dispersity PVAc oligomers is shown below (*Figure 18*.).
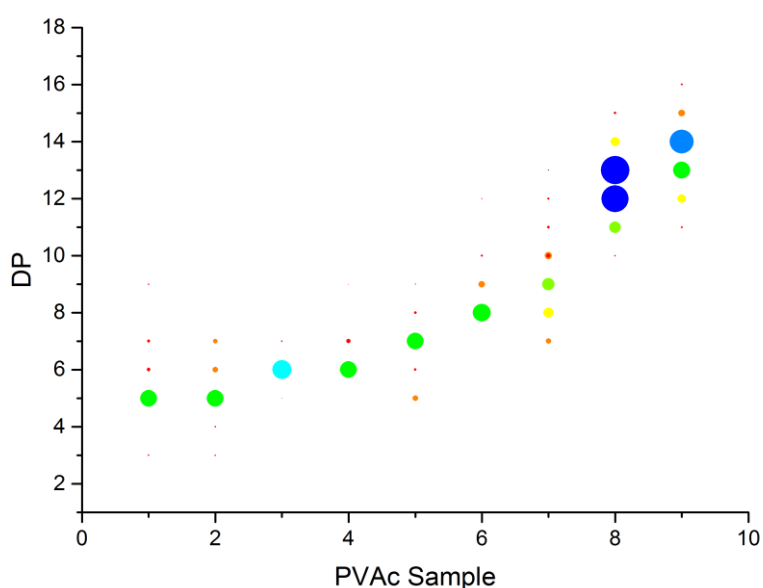
Figure 18. The final low dispersity PVAc library, obtained from separations of PVAc$_{5,10,13}$. While this graphical representation of chain length distribution is highly useful, a numerical value would also be convenient. Having ruled out dispersity as an unsuitable method of comparison between short chain polymers, a new measure was needed. The value chosen was % purity; defined as the % of the desired chain length within the whole polymer sample. For example, the percentage of DP 5 chains within a PVAc$_5$ sample. The data was once again taken from the mass spectra of the samples. The weight of peaks of each DP was combined, and the % of the nominal chain length was obtained. The % purity of the library of ultra-low dispersity PVAc oligomers is shown below (*Table 5.*).

Entry	DP^a	Label	Đ$_{m/s}$^{b}	Purity %^{c}
1	5	PVAc$_5$	1.01	62.6
2	5	PVAc$_5$	1.01	56.5
3	6	PVAc$_6$	1.005	87.8
4	6	PVAc$_6$	1.01	76.5
5	7	PVAc$_7$	1.009	57.4
6	8	PVAc$_8$	1.005	68.9
7	9	PVAc$_9$	1.01	33.0
8	12.5	PVAc$_{12.5}$	1.007	DP 12: 33.5 DP 13: 35.2
9	14	PVA$_{14}$	1.006	39.0

Table 5. % purity of PVA oligomers obtained by column chromatography. ^{a}Number degree of polymerisation, ^{b}M$_w$/M$_n$, ^{c}% of sample with chain length = DP of sample.

As well as providing a rigorous definition of the polymer samples obtained, this data also illustrates just how poorly defined even very low dispersity polymers are. For example, PVAc$_8$ only has a dispersity of 1.005, which would be considered extremely low, but is still only 68.9 % pure. This demonstrates the large degree of complexity inherent even in simple homopolymers. This complexity is only compounded further in more complicated systems such as block copolymers. This data also illustrates the bias of dispersity with increased MW. PVAc$_{14}$ has a lower dispersity than the higher purity PVA$_5$, again highlighting the limitations of dispersity as a means of comparing polymers with short chain lengths.

2.1.5 Hydrolysis of PVAc to PVA

The final synthetic stage in this investigation was conversion of the PVAc samples to PVA. Attempts to do this via hydrazine hydrate solutions proved unsuccessful due to product loss from dialysis. Attempts to dialyse the PVAc resulted in $1-2$ % yields, likely due to the very short chains dialysing out through the pores of the dialysis tubing. Therefore, we turned to sodium methoxide as a method to hydrolyse the PVAc. Excess sodium methoxide was added to PVAc *(Scheme 4.)* followed by purification by passing the product through an ion exchange column. Infrared (IR) spectroscopy (*Figure 19*) showed a complete loss of the C=O peak at 1700 cm^{-1}, confirming 100 % conversion of PVAc to PVA. ^{1}H NMR (*Figure 20., 21.*) had no residual PVAc signals, also confirming 100 % conversion.
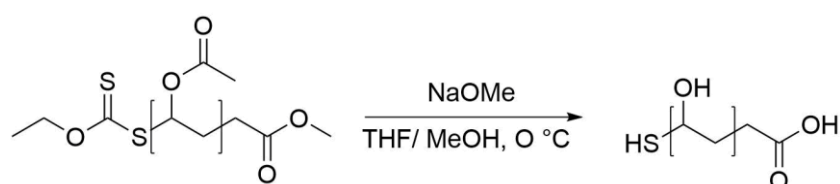
Scheme 4. Hydrolysis of PVA via sodium methoxide
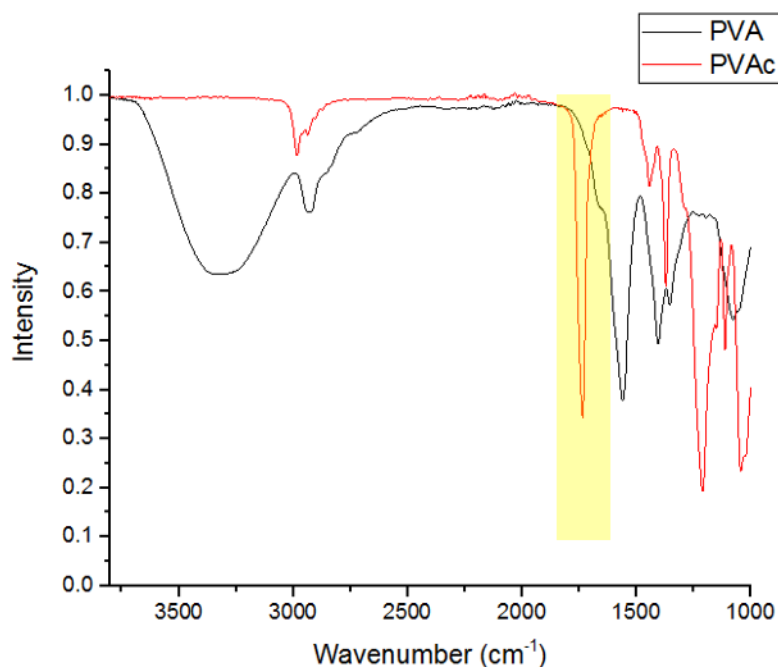
Figure 19. Overlaid IR spectra of PVA and PVAc, yellow region highlights loss of C=O
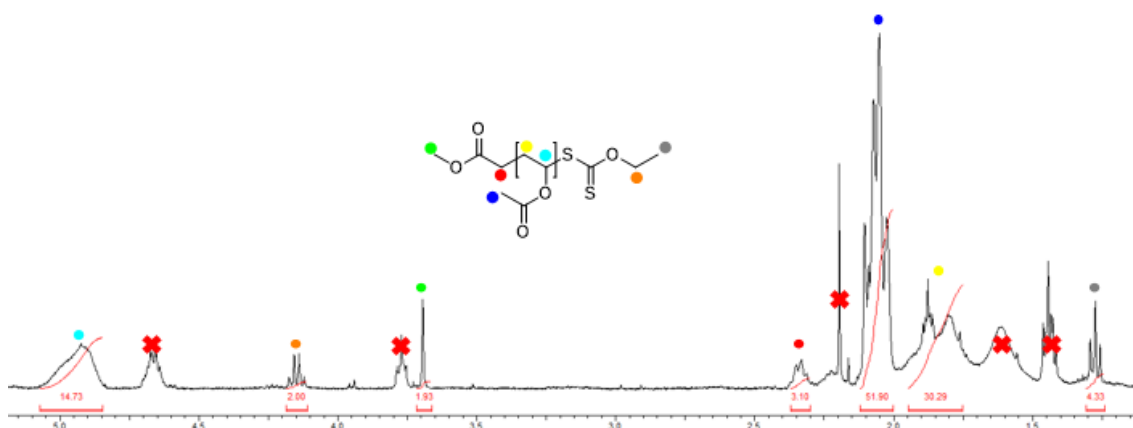
Figure 20. Representative ^1H NMR of PVAc$_{12}$ in CDCl$_3$. Residual solvent (THF/hexane) marked with crosses.
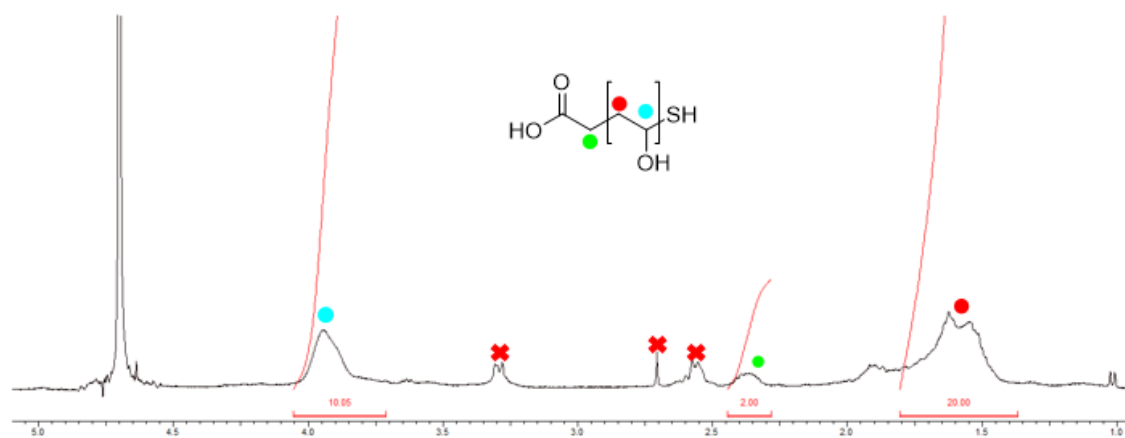
Figure 21. Representative ^1H NMR of PVA$_{10}$ in D$_2$O residual solvent (ethanol/ THF) marked with crosses.

2.2 Analysis of the IRI activity of ultra-low dispersity PVA Oligomers

2.2.1 Chain length dependence of IRI activity

With a library of fully hydrolysed, well-defined PVA oligomers to hand (*Table 6.*), the IRI activity was assessed *via* the splat assay. Briefly, a polynucleated ice wafer is created by dropping a 10 μL drop onto a glass cover slip sat on dry ice (~ - 80 °C). This results in ice crystals with diameters <10 μm, which can then be annealed (allowing them to grow) at −8 °C for 30 min before being photographed between crossed polarizers. The average size of the ice crystals with/without the additives is then compared to a PBS standard; smaller ice crystals indicate more IRI. In each case 3 repeat measurements were conducted and the ice crystal number/size was determined by manual counting. Due to the irregular shape of the ice crystals, domain recognition software fails to capture the correct information, necessitating a slower, but more accurate manual method to be employed. Initial screening of the IRI activity of the PVA oligomers at the concentrations used in previous work saw relatively low activity. No IRI activity was observed in the 0.1 – 1 mg mL^{-1} region. The first conclusion to draw was that at the chain lengths investigated (DP 5 – 14), PVA has very low IRI activity compared to the longer (RAFT-derived) PVA chains with higher dispersity, examined by Congdon.[16]

Entry	Polymer	DP	Đ	% Purity
1	PVA$_6$	6	1.005	87.8
2	PVA$_7$	7	1.009	57.4
3	PVA$_9$	9	1.01	33
4	PVA$_{12.5}$	12.5	1.007	DP 12: 33.5
				DP 13: 33.5
5	PVA$_{14}$	14	1.006	39
6	PVA$_{11}$ (*RAFT*)	11	1.14	19.12

Table 6. Library of PVA oligomers tested for IRI activity.

To facilitate comparison between the PVA samples obtained, higher concentrations were used. IRI is a concentration dependant phenomena, therefore substantially increasing the concentration sample concentration, with its subsequent activity increase, should reveal any in differences in activity between them. A concentration range of 2.5 – 50 mg mL^{-1} was found to facilitate comparison of the PVA samples obtained. To highlight the effects of separation via column chromatography, an unseparated sample of PVA (*PVA$_{11}$ (RAFT)*) (Đ = 1.14, % purity = 19.12) (*Table 6. entry 6*), was also tested.
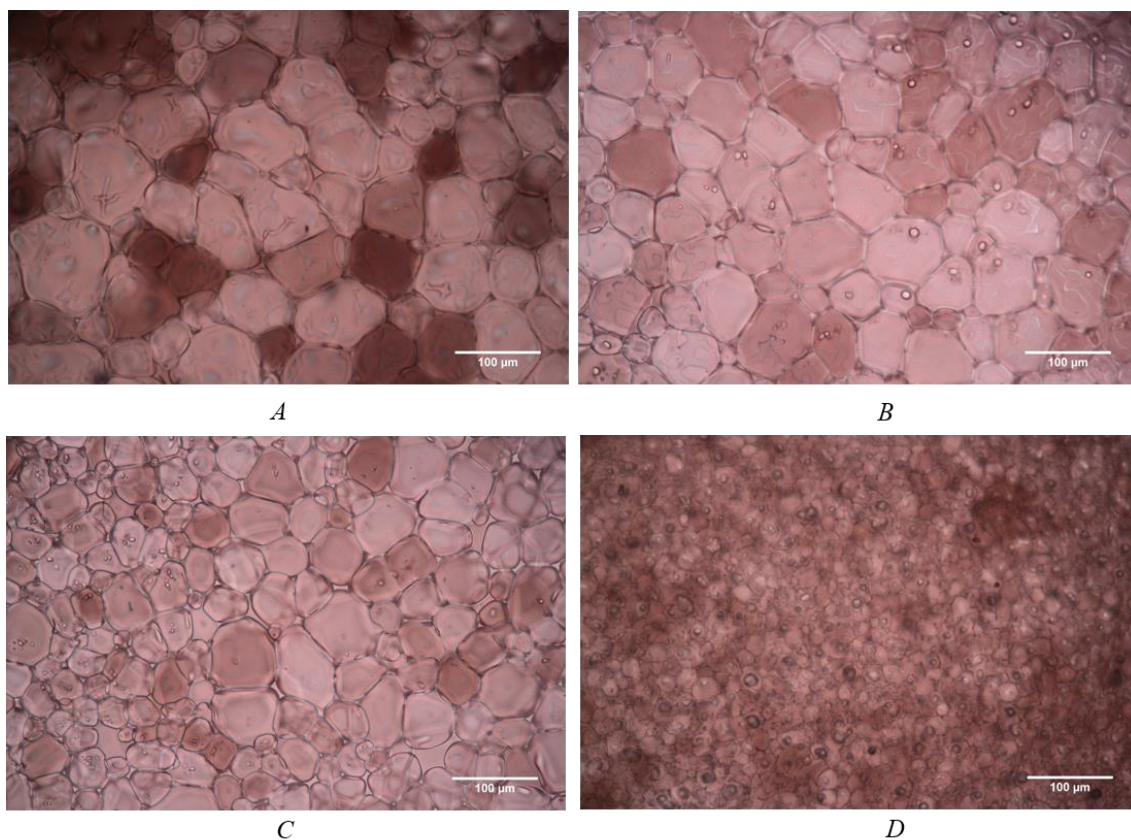
Figure 22. Micrographs 40 × zoom of (A) PBS control and 10 mg mL^{-1}PVA$_6$ (B), PVA$_{14}$ (C) and PVA$_{11}$(RAFT) (D) after annealing at – 8 ℃ for 30 mins.
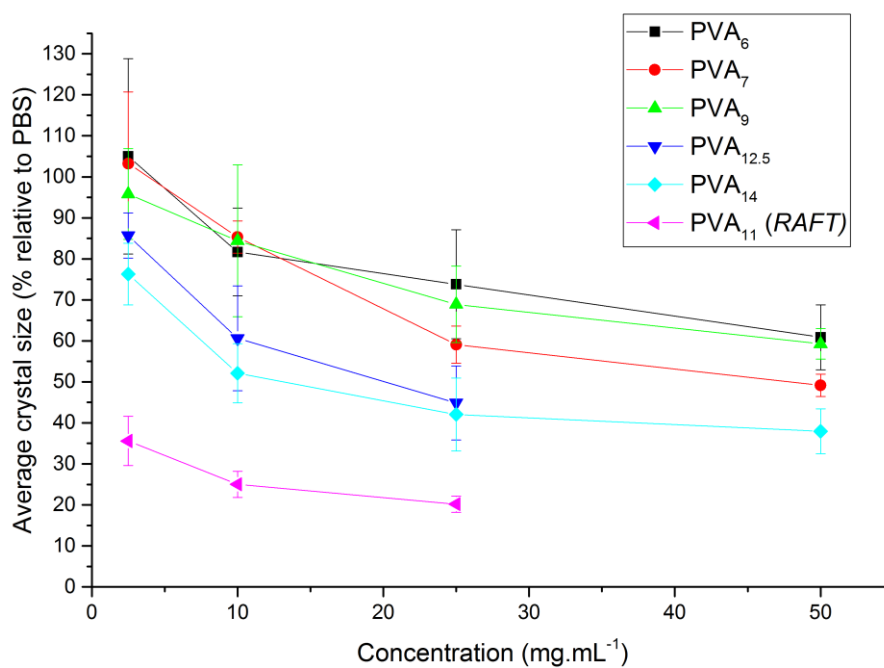
Figure 23. Ice recrystallisation inhibition activity of PVA (Table 6.) as measured by the splat assay. Error bars represent the standard deviation from at least 3 repeats.
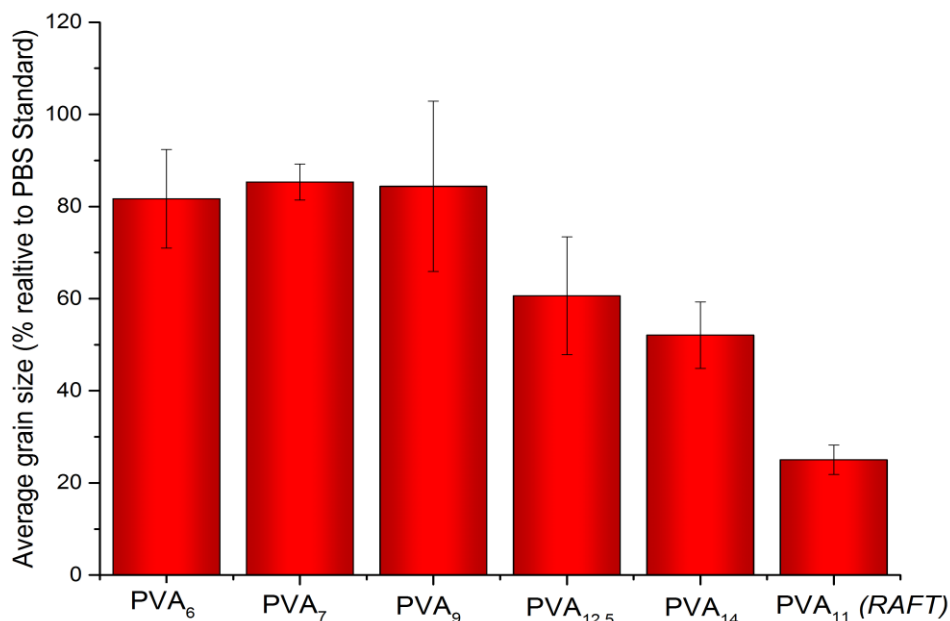
Figure 24. Summary of the ice recrystallisation inhibition activity of PVA oligomers at 10 mg mL^{-1} as measured by the splat assay. Error bars represent the standard deviation from at least 3 repeats.

Broadly, there are three levels of IRI activity visible in this data (*Figure 23.*). For ease of comparison, the data at 10 mg mL^{-1} are plotted (*Figure 24.*). At a concentration of 10 mg mL^{-1}, the following grouping is clear. PVA$_{6,7, 9}$ can be grouped into one band of IRI activity, with ~ 82 % MGS; PVA$_{12.5, 14}$ can be grouped at ~ 53 % MGS and unseparated PVA$_{11}$ *(RAFT)* gave 25 % MGS

It can be seen that PVA$_{11}$ *(RAFT)* had a significantly higher IRI activity than the ultra-low dispersity samples tested. This provides the first evidence that dispersity has a significant effect on IRI activity. From this, it can be concluded that the higher IRI activity seen in PVA$_{11}$ *(RAFT)*, and in the PVA$_{10}$ tested by Congdon *(Figure 7.)*,[22] is due to the presence of chain lengths longer than DP 14 (*Figure 25.*).

This data also demonstrates the dependence of IRI activity on chain length, as increased chain length gave higher IRI activity. It also demonstrates that IRI activity increases with the addition of 5 PVA repeat units. This is the smallest increase in PVA chain length that has resulted in increased IRI activity reported so far. No increase in IRI activity with the addition of a single repeat unit was resolvable by this assay. Budke and Koop speculated that at least 6 to 8 units were for necessary for PVA to bind to ice.[15] This data demonstrates extremely low IRI activity in 87.8 % pure DP 6 PVA and 57.4 % pure DP

7 PVA. Therefore, the ice binding model suggested by Budke and Koop, which implies IRI activity should be seen at 6 to 8 units, is likely wrong.
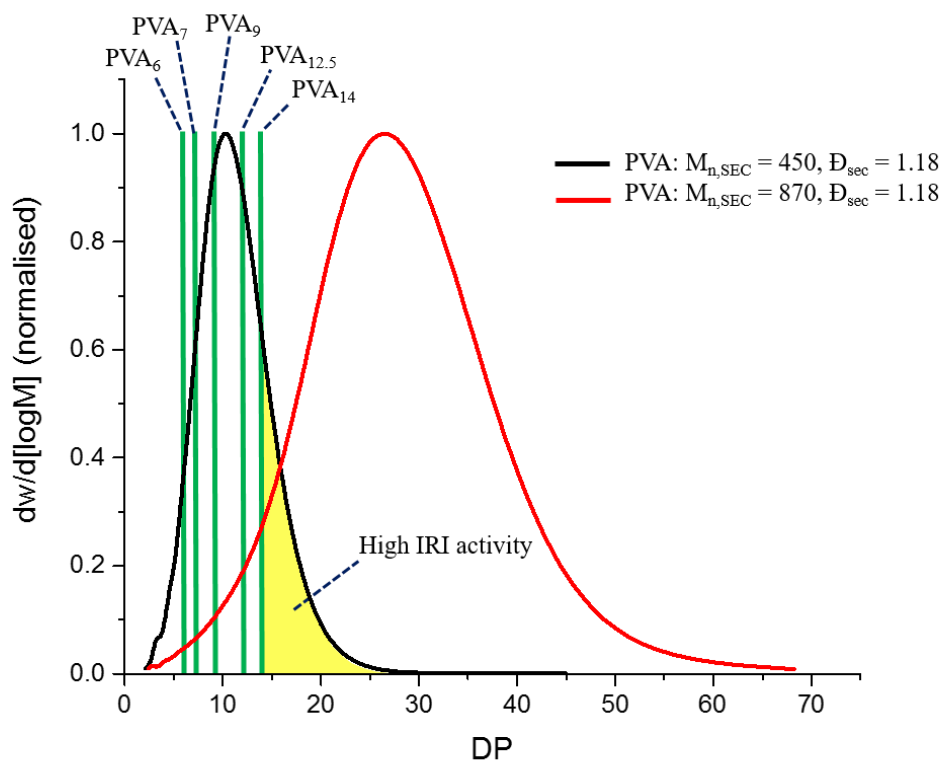
Figure 25. Comparison of ultra-low PVA oligomers and PVA samples tested by Congdon.

2.2.3 Comparison of IRI activity of short chain PVA with Poly(ols)

A key question arises from the above observation: when does PVA IRI activity deviate from that of poly-ols, which have negligible activity? Deller *et al.* have previously studied a range of oligosaccharides verses PVA, revealing that at high MW PVA has very high IRI activity, whereas IRI activity in poly-ols is extremely low and independent of MW.[17] Oligosaccharides also have a precisely defined number of hydroxyl units and are monodisperse, making them suitable comparators for this work. Using the same methods as above, glucose (a monosaccharide), lactose and trehalose (reducing and non-reducing disaccharides) which are very weak IRI's were compared in the same concentration range.
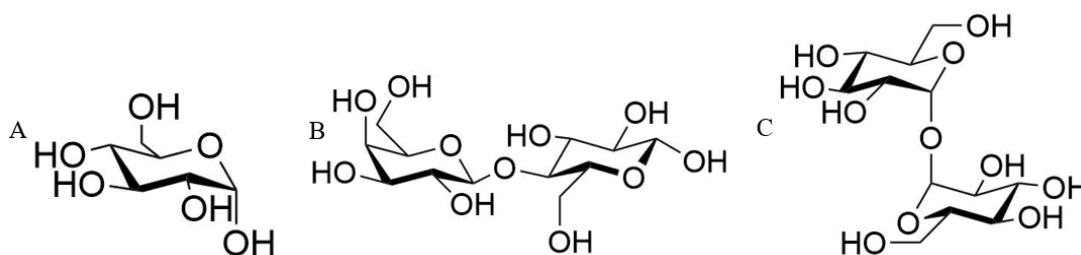
Figure 26. Chemical structure of A: glucose, B: lactose, C: trehalose.
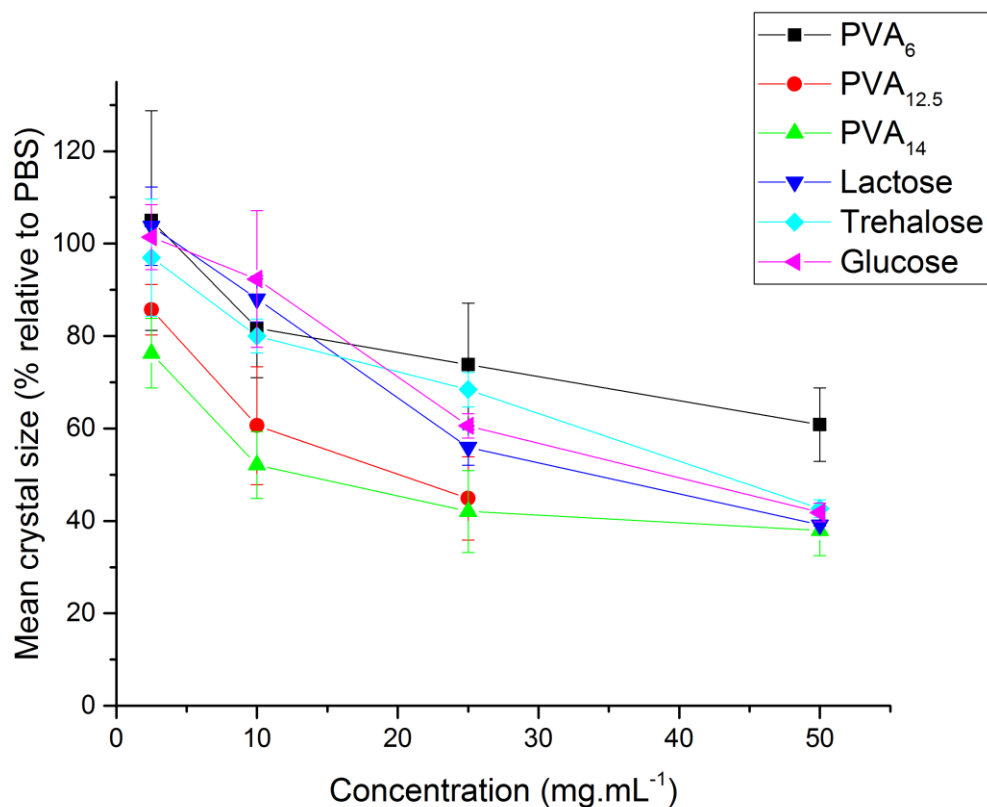
Figure 27. Comparison of IRI activity of glucose, lactose and trehalose with PVA$_6$, PVA$_{12.5}$ and PVA$_{14}$. Error bars represent the standard deviation from at least 3 repeats.

As seen in figure 27: glucose, lactose and trehalose all had essentially indistinguishable IRI activity. PVA$_{12.5}$ and PVA$_{14}$ were both more active than the poly-ols at concentrations lower than 50 mg mL^{-1}. PVA$_6$ is less active than glucose, lactose and trehalose at 25 and 50 mg.mL^{-1}, before the activities of PVA$_6$, lactose and trehalose become broadly similar at 10 and 2.5 mg mL^{-1}. See appendix A.9 for micrographs.

It is clear that PVA$_{12.5}$ and PVA$_{14}$ are more active than glucose, lactose and trehalose. In contrast, PVA$_6$ is less active. The work of Deller states that poly-ols have the same IRI activity no matter the degree of hydroxylation. Here, a significant increase in PVA IRI activity with increased number of OH groups (from PVA$_6$ to PVA$_{12.5}$) is observed in comparison to the poly-ols tested; despite the number of OH groups in PVA$_{12.5}$ and PVA$_{14}$ still being relatively low. This seems to be an observation of activity in PVA 'switching on'; i.e. PVA$_6$ and the poly-ols are IRI active via a poly-ol like mechanism. In contrast, it is clear that the IRI activity of PVA$_{12.5}$ and PVA$_{14}$, even at these short chain lengths is a surprisingly high. The IRI activity observed does not seem to be due to PVA behaving like a, poly-ol but something more complex.

From a structural perspective: glucose, lactose and trehalose have a cyclic conformation. The OH groups have precise locations within the ring structure of each molecule and cannot freely rotate. In contrast, OH groups in PVA are free to move around and whole chain can contort. This lack of defined conformation may allow PVA to bind to ice more effectively than the poly-ol molecules tested. As observed, this effect is not potent relative to poly-ol molecules until a chain length of 12.5 is reached. However, this fairly straightforward explanation is limited by the poor IRI activity of glycopolymers tested by Gibson.[49] These have flexible chains and OH groups but are not strongly IRI active, providing further evidence of the complexity of the IRI mechanism of PVA. All the current evidence regarding the PVA-IRI structure activity relationship is summarised below (*Table 7.*)

Structural modification to PVA	Effect on IRI activity
Increased MW	Increase
Increase from DP 10 – DP 19 (Đ=1.18)	Significant increase
Increased hydrophobic character	Decrease
Increased hydrophilic character	Up to 20% PVP tolerated before decrease
Addition of pendant methyl to main chain	Small decrease
Hydrophobic block copolymer	No change
Ultra-low Đ PVA_{5-14}	Low activity
Increase from DP 6-DP 14 (Đ very low)	Low activity, increase in activity compared to poly-ols.

Table 7. A summary of the structure – activity relationships of PVA – IRI

3. Conclusion

A technique to access low dispersity oligomers of PVAc and PVA was developed. A series of low MW PVAc samples were made *via* RAFT polymerisation. They were then separated by column chromatography. From this, a library of ultra-low dispersity PVAc oligomers between DP 5 and DP 14 was assembled. These polymers were rigorously defined by graphical visualisation of the chain length distribution within the samples and by measuring the % purity. This PVAc library was then hydrolysed to PVA.

The IRI activity of select PVA oligomers was tested. Across the full range of chain lengths the ultra-low dispersity oligomers were inactive compared to higher MW samples tested in previous work. This was the first demonstration of the effect of dispersity on the IRI activity of PVA, with higher dispersity being associated with higher IRI activity. IRI activity increased between DP 5 and DP 14 PVA, demonstrating that very small increases in chain length result in more IRI activity.

The IRI activity of the ultra-low dispersity oligomers was then compared to a series of poly-ols. It was found that DP 6, 7 and 9 PVA were either less active or the equally active as the poly-ols, depending on concentration. $PVA_{12.5}$ was more active. This gave evidence for a 'switching on' of IRI activity in PVA, as the IRI activity for $PVA_{12.5}$ was higher than observed for poly-ols.

The mechanism of action behind the erroneously high IRI activity of PVA remains tantalisingly out of reach. While some evidence of the 'switch on' region has been found in this study, the chain length where IRI significantly increases was inaccessible with this approach.

This study focussed on chain length and dispersity as determinants of IRI activity. Future work in this area could revolve around a stepwise synthesis of PVA, testing IRI with each successive repeat unit addition until the significant activity jump reported by Congdon is observed. Other considerations, such as the effect of tacticity on IRI activity could be investigated, through use of a chiral CTA to obtain PVA of defined tacticity. The structural features that contribute towards the IRI acitivity of PVA still need to be elucidated if the rational design of macromolecular antifreeze agents is to be realised.

4. Materials and Analytical Methods

4.1 Materials

Phosphate-buffered saline (PBS) solutions were prepared using preformulated tablets (Sigma-Aldrich) in 200 mL of Milli-Q water (>18.2 Ω mean resistivity) to give [NaCl] = 0.138 M, [KCl] = 0.0027 M, and pH 7.4. Vinyl acetate was purchased from Sigma-Aldrich and was filtered through a silica plug to remove inhibitors prior to use. 4,4′-Azobis(4-cyanovaleric acid) (ACVA) was recrystallized from methanol and stored at −8 °C in the dark. Amberlite ion exchange resin was purchased from Sigma-Aldrich. All solvents were purchased from VWR or Sigma-Aldrich and used without further purification.

4.2 Physical and Analytical Methods

^{1}H and ^{13}C NMR spectra were recorded on Bruker DPX-300 and DPX-400 spectrometers using deuterated solvents obtained from Sigma-Aldrich. Chemical shifts are reported relative to residual nondeuterated solvent. Mass spectral analyses were obtained using Bruker MicroTOF electrospray instruments using positive or negative electrospray mode. FTIR spectra were acquired using a Bruker Vector 22 FTIR spectrometer with a Golden Gate diamond attenuated total reflection cell.

Where applicable, Gel permeation chromatography (GPC) was used to obtain molecular weights and dispersities of synthesized polymers. The THF GPC system comprised of an Agilent 390-LC MDS instrument equipped with differential refractive index (DRI) and dual wavelength UV detectors. The system was equipped with 2 x PLgel Mixed C columns (300 x 7.5 mm) and a PLgel 5 µm guard column. The eluent is THF with 2 % TEA (triethylamine) and 0.01 % BHT (butylated hydroxytoluene) additives. Samples were run at 1mL min at 30 °C. Poly(methyl methacrylate) and polystyrene standards (Agilent EasyVials) were used for calibration. Analyte samples were filtered through a GVHP membrane with 0.22 µm pore size before injection. Respectively, experimental molar mass (M_n, SEC) and dispersity values of synthesized polymers were determined by conventional calibration using Agilent GPC/SEC software.

Ice wafers were annealed on a Linkam Biological Cryostage BCS196 with T95-Linkpad system controller equipped with a LNP95-Liquid nitrogen cooling pump, using liquid nitrogen as the coolant (Linkam Scientific Instruments UK, Surrey, U.K.). An Olympus CX41 microscope equipped with a UIS-2 20x/0.45/∞/0−2/FN22 lens (Olympus Ltd., Southend on sea, U.K.) and a Canon EOS 500D SLR digital camera were used to obtain

all images. Image processing was conducted using Image J, which is freely available from http://imagej.nih.gov/ij/.

5. Experimental

5.1 Synthesis of methyl (ethoxy carbonothioyl) sulfanyl acetate (CTA 1)
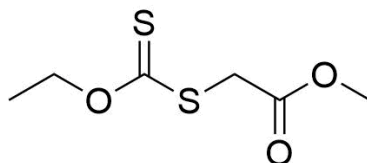
Ethanol (140 mL) was added to a round bottomed flask equipped with a stirrer bar. Potassium hydroxide (22.9 g, 0.41 mol) was added and left to dissolve for 1 h. Carbon disulphide (24.2 mL, 0.40 mol) was then added dropwise, forming a yellow solution that was left to stir for 5 h. Methyl bromoacetate (13 mL, 0.012 mol) was added dropwise and the solution left to stir overnight. The solution was washed with cold ethanol then filtered and concentrated *in vacuo*. The crude product was partitioned in a DCM and saturated brine solution; the organic fraction then concentrated *in vacuo*. This product was then dissolved in ethyl acetate and filtered to remove impurities. Finally the product was concentrated *in vacuo* and thoroughly dried under vacuum. Yield 9.10 g 39 %. ^{1}H NMR (400 MHz, CDCl$_3$): δ = 1.44 (2H, t, CH$_3$CH_2), 3.78 (3H, s, CH_3O), 3.93 (2H, d, SCH_2), 4.67 (3H, q, CH_3CH$_2$). ^{13}C NMR (CDCl$_3$): δ = 13.7 (CH$_2$-CH$_3$), 37.9 (S-CH$_2$), 61.9 (CO$_2$-CH$_3$), 70.6 (CH$_2$-CH$_3$), 167.8 (C=O), 212.6 (C=S). Other peaks due to solvent (ethanol).

5.2 Polymerisation of vinyl acetate using CTA 1

As a representative example: poly(vinyl acetate (5 g, 58 mmol), was filtered three times through a silica plug. The vinyl acetate, CTA 1 (0.062 , 0.29 mmol) and ACVA ((4,4' azobis(4-cyanovaleric acid); 8.13 mg, 0.029 mmol) was then added to a stoppered vial containing a stirrer bar. The solution was degassed under N$_2$ for 20 minutes before being left to polymerise for typically 18 h. The resulting yellow solid was dissolved in a 1:1 mixture of THF (tetrahydrofuran) and hexane and the polymer precipitated via centrifugation three times, decanting off the hexane each time. The final polymer was recovered as a sticky yellow solid after drying under vacuum. Representative characterisation data for PVAc$_{150}$: ^{1}H NMR (400 MHz, CDCl$_3$) δ = 2.06 (3H, br, COCH_3), 1.87 (2H, br, CH_2) 4.88 (1H, br, CHOCH$_2$); M_n^{SEC}(THF) = 15000 Da, Đ = 1.65.

5.3 Separation of poly(vinyl acetate) oligomers *via* column chromatography

As a representative example: 10 g of vinyl acetate (DP NMR ≈ 6) was loaded onto a silica column (6.5 cm diameter, 20 cm silica gel). Vinyl acetate oligomers were separated using a 75:25 ethyl acetate: hexane solvent. 80 fractions of approximately 20 mL were obtained. Fractions were taken until no separation could be seen *via* TLC. TLC spots were visualised under long wave UV light or by brief immersion in potassium permanganate solution followed by heating. The fractions were dried *in vacuo*. The mass spectrum of each fraction was obtained and used to determine Đ and purity %.

5.4 Hydrolysis of poly(vinyl acetate) to poly(vinyl alcohol)

As a representative example: vinyl acetate (0.152 g), ethanol (15 mL) and THF (5 mL) was added to a round bottomed flask equipped with a stirrer bar. The solution was cooled over ice. Sodium methoxide (1 mL, 0.018 mol) was added dropwise forming a deep orange solution, the reaction was allowed to proceed for one hour. The solution was then neutralised by passing through a column packed with Amberlite ion exchange resin until a neutral pH was reached. The product was then dried *in vacuo*, before dissolving in deionised water and freeze drying. Impurities were removed by dissolving the freeze dried product in deionised water and filtering off any undissolved solids before freeze drying again. The final product was obtained as a brown powder. Representative characterisation data for PVA (DP (NMR) ≈ 12, Đ 1.008): ^{1}H NMR (400 MHz, D$_2$O) δ = 1.62 (2H, br, CH_2), 3.95 (1H, br, CHOH).

5.6 Ice recrystallisation inhibition 'splat' assay

A droplet of polymer containing PBS solution was dropped from 2 m onto a glass slide cooled to -78 °C using dry ice. On impact with the glass, the droplet spreads out and freezes instantly, forming a single layer of ice crystals. The wafer is then placed in a liquid nitrogen cooled cryostage held at – 8 °C. Micrographs of the ice crystals are taken at 20 x, 10 x and 4 x zoom under cross polarisers, the wafer is then left to anneal for another 30 minutes. Three further micrographs at 20 x, 10 x and 4 x zoom are taken at this point. The photos are then analysed using Image J to determine the average crystal size. The average crystal size is obtained by counting the crystals visible in the photo and dividing by the area of the photo (determined using a standard of 100 µm wide gold tracks printed on a glass slide). This value is averaged across three repeats and then compared to a standard PBS solution giving the average crystal size compared to PBS as a %.

6. References

1   A. L. DeVries, *Science.*, 1971, **172**, 1152–1155.

2   K. V. Ewart, Q. Lin and C. L. Hew, *Cell. Mol. Life Sci.*, 1999, **55**, 271–283.

3   S. S. Mallajosyula, K. Vanommeslaeghe and A. D. Mackerell, *J. Phys. Chem. B*, 2014, **118**, 11696–11706.

4   M. Griffith and K. V. Ewart, 1995, **13**, 375–402.

5   A. P. Esser-Kahn, V. Trang and M. B. Francis, *J. Am. Chem. Soc.*, 2010, **132**, 13264–13269.

6   P. Kim, T. S. Wong, J. Alvarenga, M. J. Kreder, W. E. Adorno-Martinez and J. Aizenberg, *ACS Nano*, 2012, **6**, 6569–6577.

7   K. G. M. Brockbank, L. H. Campbell, E. D. Greene, M. C. G. Brockbank and J. G. Duman, *Vitr. Cell. Dev. Biol. Anim.*, 2011, **47**, 210–217.

8   M. I. Gibson, *Polym. Chem.*, 2010, **1**, 1141.

9   A. Chakrabartty, D. S. Yang and C. L. Hew, *J. Biol. Chem.*, 1989, **264**, 11313–11316.

10   W. Zhang and R. A. Laursen, *FEBS Lett.*, 1999, **455**, 372–376.

11   L. Ratke and P. W. Voorhees, *Growth and Coarsening: Otswald Ripening in Material Processing*, Springer - Verlag, Berlin, 2002.

12   C. A. Knight, D. Wen and R. A. Laursen, *Cryobiology*, 1995, 32, 23–34.

13   T. Inada and S. S. Lu, *Chem. Phys. Lett.*, 2004, **394**, 361–365.

14   T. Wang, Q. Zhu, X. Yang, J. R. Layne and A. L. Devries, *Cryobiology*, 1994, **31**, 185–192.

15   C. Budke and T. Koop, *ChemPhysChem*, 2006, **7**, 2601–2606.

16   T. Congdon, R. Notman and M. I. Gibson, *Biomacromolecules*, 2013, **14**, 1578–1586.

17   R. Deller, T. Congdon, M. Sahid, M. Morgan, M. Vatish, D. A. Mitchell, R. Notman and M. I. Gibson, *Biomater. Sci.*, 2013, **1**, 478–485.

18   T. Congdon, P. Shaw and M. I. Gibson, *Polym. Chem.*, 2015, **6**, 4749–4757.

19   T. R. Congdon, R. Notman and M. I. Gibson, *Biomacromolecules*, 2016, **17**, 3033–3039.

20   R. C. Deller, J. E. Pessin, M. Vatish, D. A. Mitchell and M. I. Gibson, *Biomater. Sci.*, 2016, **47**, 935–945.

21   T. Takaaki and S.-S. Lu, *Cryst. Growth Des.*, 2003, **3**, 747–752.

22   D. J. Phillips, T. R. Congdon and M. I. Gibson, *Polym. Chem.*, 2016, **7**, 1–13.

23   R. C. Deller, M. Vatish, D. A. Mitchell and M. I. Gibson, *Nat. Commun.*, 2014, **5**, 3244.

24   R. C. Deller, M. Vatish, D. A. Mitchell and M. I. Gibson, *ACS Biomater. Sci. Eng.*, 2015, **1**, 789–794.

25   D. E. Mitchell, N. R. Cameron and M. I. Gibson, *Chem. Commun.*, 2015, **51**, 12977–80.

26   C. Stubbs, J. Lipecki and M. I. Gibson, *Biomacromolecules*, 2017, **18**, 295–302.

27   K. Matsumura and S. Hyon, *Biomaterials*, 2009, **30**, 4842–4849.

28   R. Rajan, F. Hayashi, T. Nagashima and K. Matsumura, *Biomacromolecules*, 2016, **17**, 1882–1893.

29   A. K. Balcerzak, C. J. Capicciotti, J. G. Briard and R. N. Ben, *RSC Adv.*, 2014, **4**, 42682–42696.

30   A. Eniade, M. Purushotham, R. N. Ben, J. B. Wang and K. Horwath, *Cell Biochem. Biophys.*, 2003, **38**, 115–124.

31   C. J. Capicciotti, J. D. R. Kurach, T. R. Turner, R. S. Mancini, J. P. Acker and R. N. Ben, *Sci. Rep.*, 2015, **5**, 9692.

32   C. J. Capicciotti, R. S. Mancini, T. R. Turner, T. Koyama, M. G. Alteen, M. Doshi, T. Inada, J. P. Acker and R. N. Ben, *ACS Omega*, 2016, **1**, 656–662.

33   G. Odian, *Principles of Polymerization*, Wiley-Interscience, Hoboken, 2004.

34   S. Mori and H. Barth, *Size Exclusion Chromatography*, Springer - Verlag Berlin Heidelberg, 1999.

35   H. Zhu, T. Yalcin and L. Li, *J. Am. Soc. Mass Spectrom.*, 1998, **9**, 275–281.

36 S. Harrisson, X. Liu, J.-N. Ollagnier, O. Coutelier, J. D. Marty and M. Destarac, *Polymers (Basel).*, 2014, **6**, 1437–1488.

37 S. Perrier and P. Takolpuckdee, *J. Polym. Sci. Part A Polym. Chem.*, 2005, **43**, 5347–5393.

38 J. Lawrence, S. H. Lee, A. Abdilla, M. D. Nothling, J. M. Ren, A. S. Knight, C. Fleischmann, Y. Li, A. S. Abrams, B. V. K. J. Schmidt, M. C. Hawker, L. A. Connal, A. J. McGrath, P. G. Clark, W. R. Gutekunst and C. J. Hawker, *J. Am. Chem. Soc.*, 2016, **138**, 6306–6310.

39 L. Martin, G. Gody and S. Perrier, *Polym. Chem.*, 2015, **6**, 4875–4886.

40 J. Chiefari, Y. K. B. Chong, F. Ercole, J. Krstina, J. Jeffery, T. Le, R. Mayadunne, G. F. Meijs, C. L. Moad, G. Moad, E. Rizzardo, S. H. Thang and C. South, *Macromolecules*, 1998, **31**, 5559–5562.

41 M. E. Levere, I. Willoughby, S. O'Donohue, A. de Cuendias, A. J. Grice, C. Fidge, C. Remzi Becer and D. M. Haddleton, *Polym. Chem.*, 2010, **1**, 1086–1094.

42 J. D. Moskowitz, B. A. Abel, C. L. McCormick and J. S. Wiggins, *J. Polym. Sci. Part A Polym. Chem.*, 2016, **54**, 553–562.

43 D. Held and P. Kilz, *Macromol. Syposia*, 2006, **231**, 145–165.

44 L. S. Litvinova and N. G. Bel'nikevich, *Polym. Sci. Ser. A*, 2010, **52**, 1250–1256.

45 L. Albertin and N. R. Cameron, *Macromolecules*, 2007, **40**, 6082–6093.

46 R. R. Chance, S. P. Baniukiewicz, D. Mintz, G. Ver Strate and N. Hadjichristidis, *Int. J. Polym. Anal. Charact.*, 1995, **1**, 3–34.

47 B. Thomson and K. Suddaby, *Eur. Polym. J.*, 1996, **32**, 239–256.

48 B. O. Keller, J. Sui, A. B. Young and R. M. Whittal, *Anal. Chim. Acta.*, 2008, **627**, 71–81.

49 M. I. Gibson, C. A. Barker, S. G. Spain, L. Albertin and N. R. Cameron, *Biomacromolecules*, 2009, **10**, 328–333.

7. Appendix

A.1
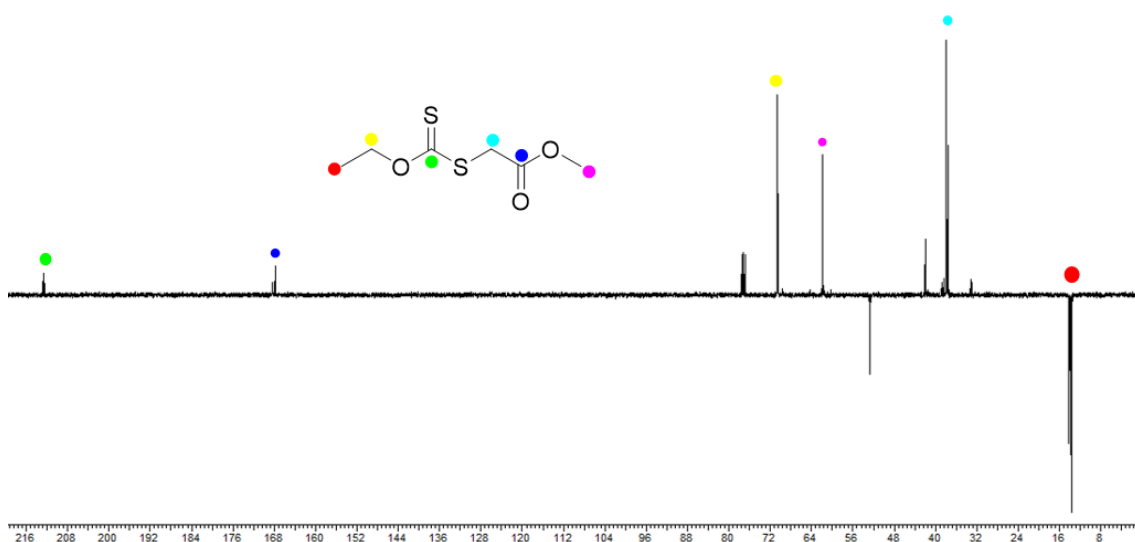
Fig A.1 ^{13}C NMR of MADIX 1.

A.2
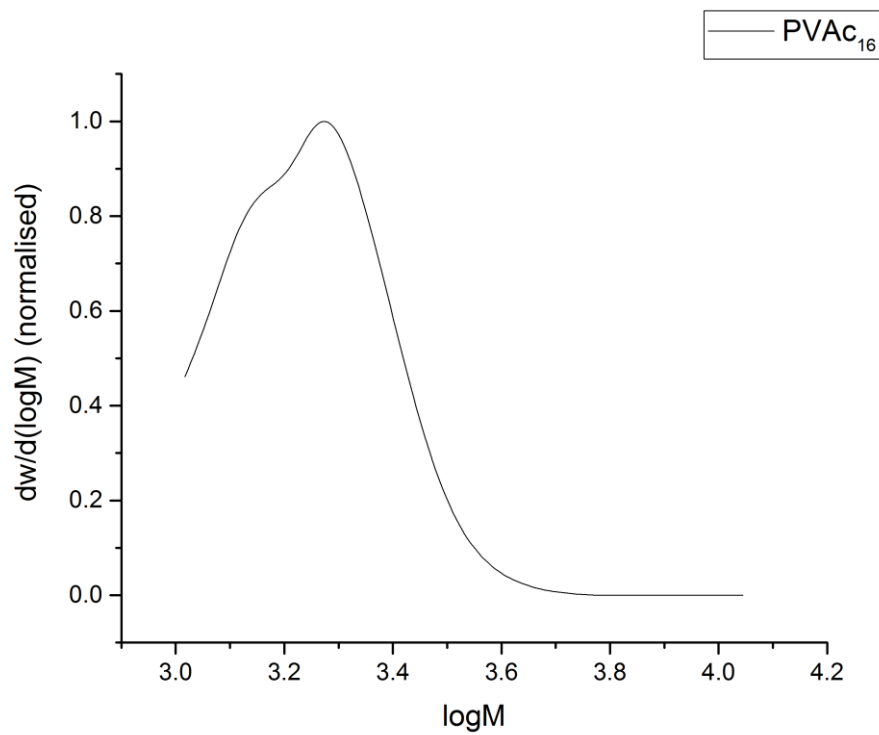
A.2 GPC THF Trace of PVAc$_{16}$

A.3
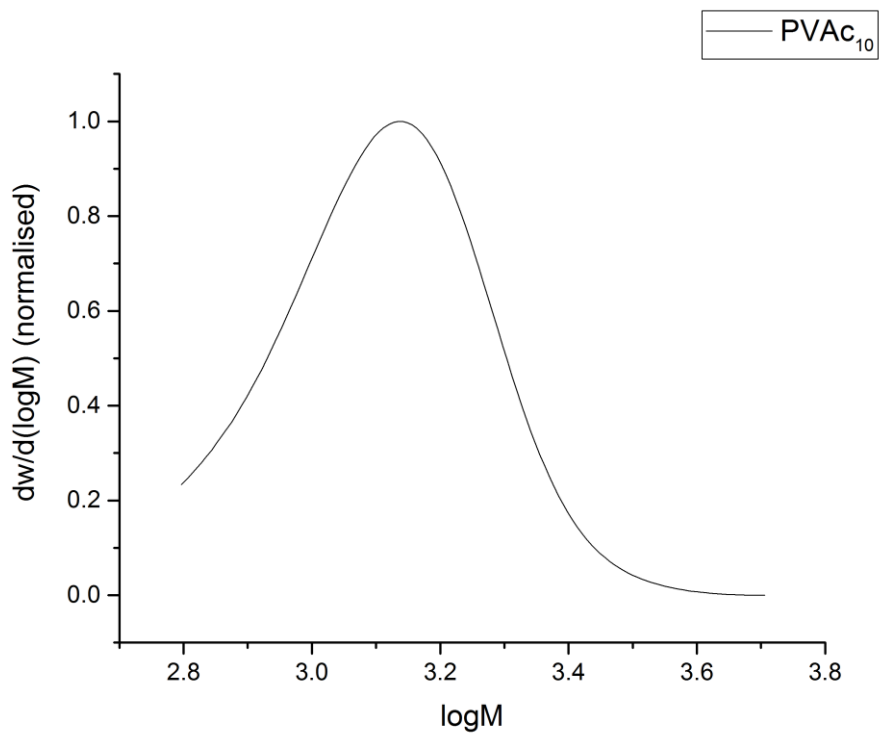
A.3 GPC THF Trace of PVAc₁₀

A.4
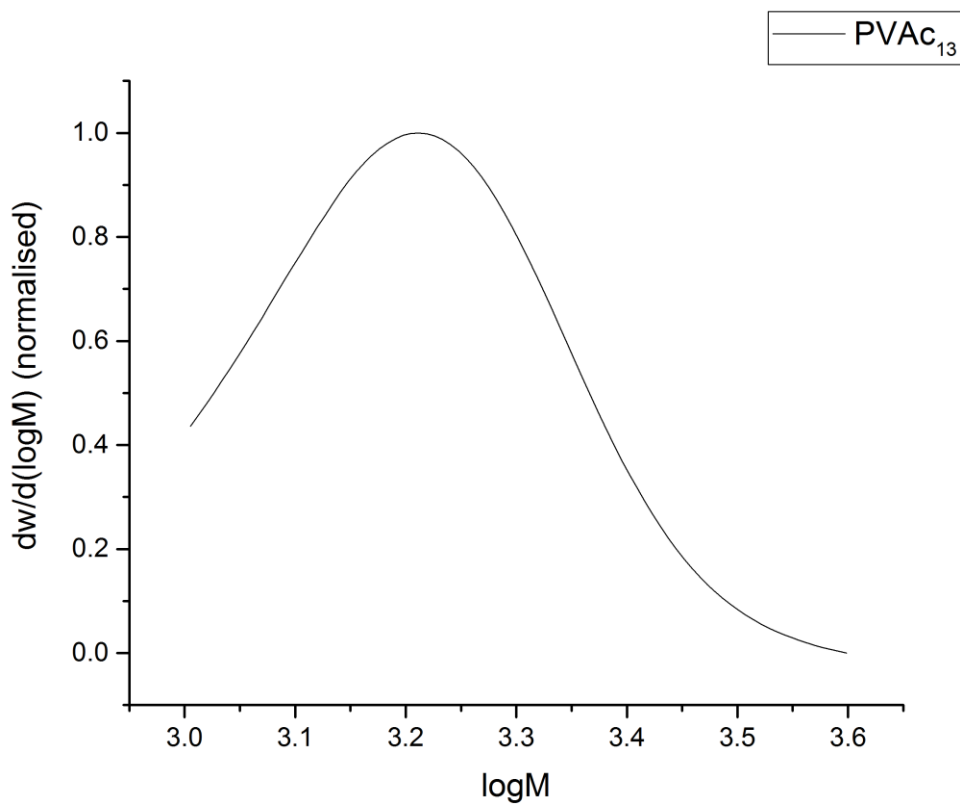
A.4 GPC THF trace of PVAc₁₃

A.5 Dispersity from mass spectrum

$$M_i = peak\ intensity \qquad (A.6.1)$$

$$N_i = M_i \times peak\ intensity \qquad (A.6.2)$$

$$M_n = \frac{\sum N_i\, M_i}{\sum N_i} \qquad (A.6.3)$$

$$M_w = \frac{\sum N_i M_i^2}{\sum N_i\, M_i} \qquad (A.6.4)$$

$$\DJ = \frac{M_w}{M_n} \qquad (A.6.5)$$

A.6 obtaining chain length distribution from mass spectrum

Fully assign mass spectrum. Obtain weight for each chain length. Plot bubble graph of weight of each chain length.

A.7 % Purity from mass spectrum

Fully assign mass spectrum. Obtain weight for each chain length.

$$\%\ purity = \frac{\sum weight\ of\ desired\ chain\ length}{\sum weight\ of\ all\ chain\ lengths} \times 100 \qquad (A.7.1)$$

A.8
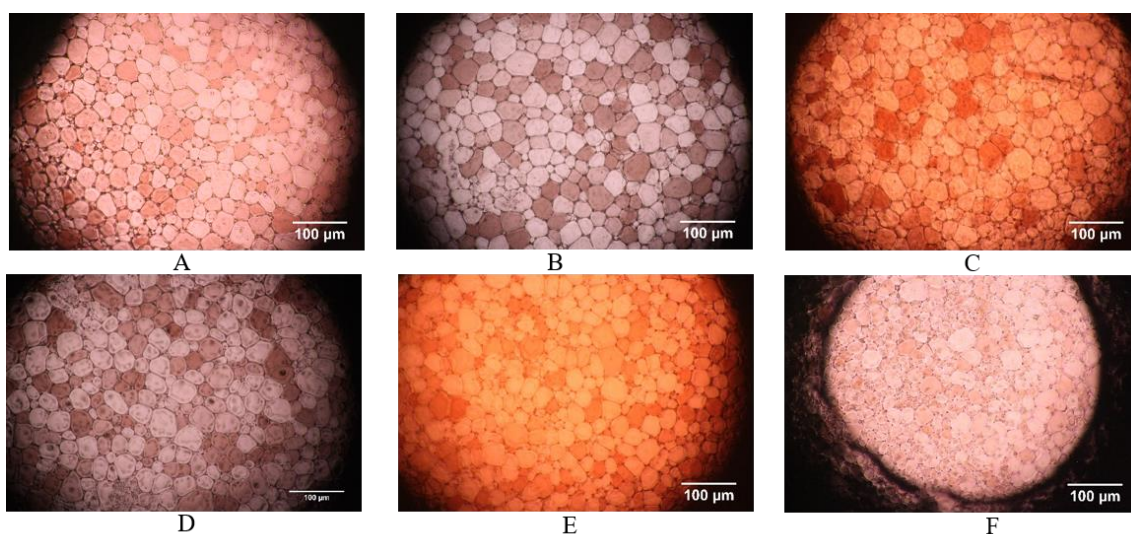
Fig A.9 Micrographs at 20 × zoom of 10 mg mL^{-1} solutions of (A) PVA$_6$, (B) trehalose, (C) lactose, (D) PVA$_{12.5}$ and (E) PVA$_{14}$ after annealing at − 8 °C for 30 mins.

A.9
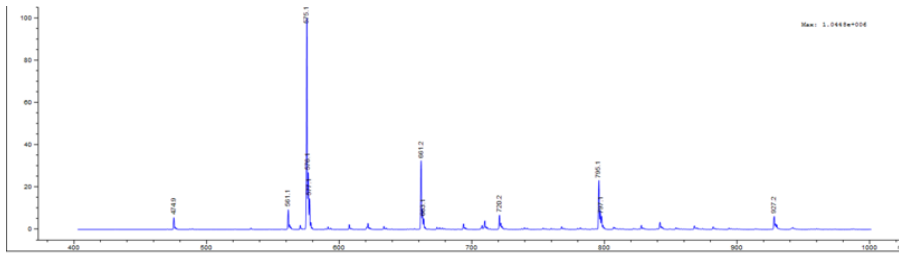
A.9.1 PVAc$_5$
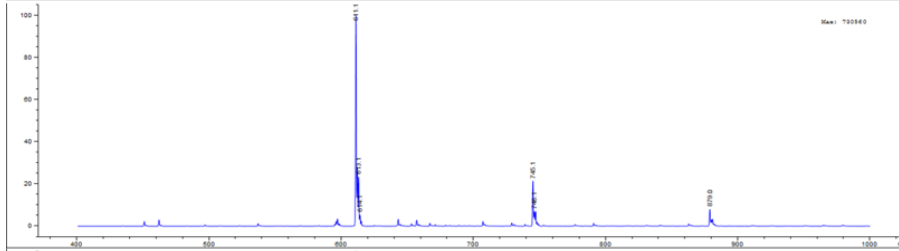
A.9.2 PVAc$_6$
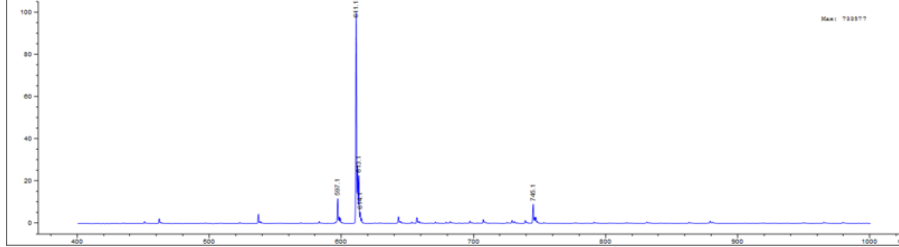
A.9.3 PVAc$_6$
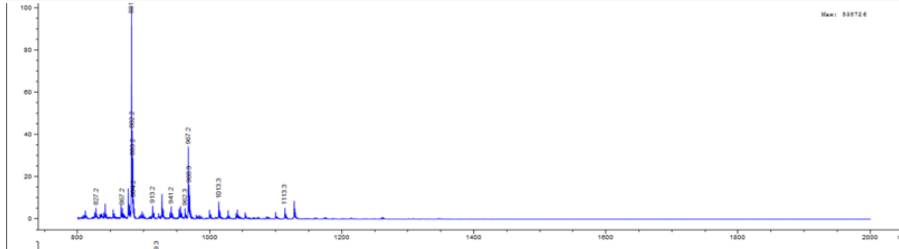
A.9.4 PVAc$_7$
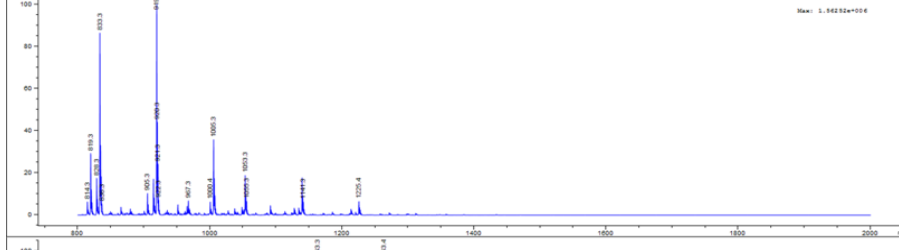
A.9.5 PVAc$_9$
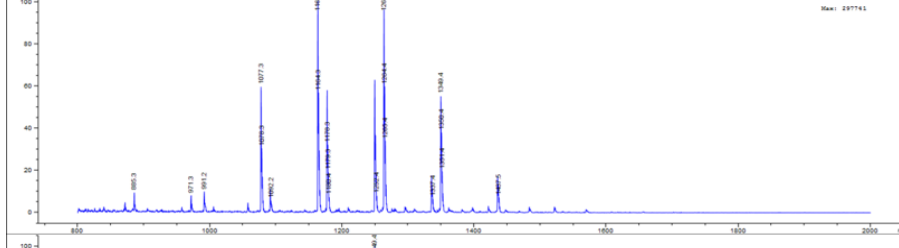
A.9.6 PVAc$_{12.5}$
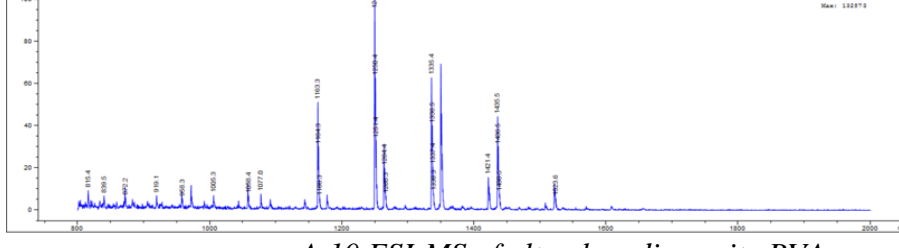
A.9.7 PVAc$_{14}$

A.10 ESI-MS of ultra-low dispersity PVAc.